Medizinische Fakultät

der

Universität Duisburg-Essen

Aus der Klinik für Neurologie

Consequences of experimentally induced *Streptococcus pneumoniae* pneumonia for post-ischemic neurological recovery, ischemic injury and brain remodeling

I n a u g u r a l d i s s e r t a t i o n

zur

Erlangung des Doktorgrades der Medizin

durch die Medizinische Fakultät

der Universität Duisburg-Essen

Vorgelegt von

Dongpei Yin

aus Hebei, China

2024

DOI: 10.17185/duepublico/82723
URN: urn:nbn:de:hbz:465-20241211-075216-5

Dekan: Herr Univ.-Prof. Dr. med. J. Buer

Gutachter/in: Herr Univ.-Prof. Dr. med. D. M. Hermann

Gutachter/in: Frau Priv.-Doz. Dr. phil. J. Herz

Gutachter/in: Frau Univ.-Prof. L. Klotz

Tag der mündlichen Prüfung: 25. November 2024

PUBLICATION

This thesis is mostly based on the manuscripts in preparation：

Yin, D., Wang, C., Singh, V., Tuz, A., Doeppner, T. R., Gunzer, M. & Hermann, D. M. Delayed DNase-I administration, but not gasdermin-D inhibition induces brain hemorrhage formation after transient focal cerebral ischemia in mice. (Revised)

Yin, D., Siebels, B., Siemes, D., Thiebes, S., Pylaeva, E., Schlueter H., Shevchuk, O., Wang, C., Qi, Y., Singh, V., Tuz, A., Hagemann, N., Mohamud Yusuf, A., Dzyubenko, E., Kaltwasser, B., Tertel, T., Popa-Wagner, A., Doeppner, T. R., Giebel, B., Engel, D. R., Jablonska, J., Gunzer, M. & Hermann, D. M. Consequences of experimentally induced Streptococcus pneumoniae pneumonia for post-ischemic neurological recovery, ischemic injury and brain remodeling. (In preparation)

Contents

1. INTRODUCTION 7

1.1. Epidemiology of stroke 7

1.2. Pathophysiology of ischemic stroke 7

1.3. Current status and exploration of therapies for ischemic stroke 8

1.4. Stroke-associated pneumonia 9

1.5. Role of neutrophils in ischemic stroke and pneumonia 12

1.6. Aim of the study 13

2. MATERIALS AND METHODS 14

2.1. Legal issues, animal housing, randomization and blinding 14

2.2. Focal cerebral ischemia 14

2.3. Animal allocation 16

2.4. *Streptococcus pneumoniae* culture and pneumonia induction 18

2.5. Drug administration 19

2.6. Neurological deficit score 20

2.7. Behavioral tests 24

2.8. Measurement of infarct volume, brain edema, brain atrophy and brain hemorrhage 26

2.9. Immunohistochemistry 26

2.10. Microglia/macrophage morphology analysis 29

2.11. Flow cytometry 29

2.12. Quantification of NETs in mouse plasma samples 31

2.13. Statistical data analysis 32

3. RESULTS 33

3.1. Post-stroke pneumonia exacerbates neurological deficits, brain edema, and IgG extravasation in the acute stroke phase 33

3.2. Post-stroke pneumonia aggravates peripheral leukocyte infiltration and microvascular ICAM-1 expression 35

3.3. Post-stroke pneumonia increases the formation of microthrombi 37

3.4. Post-stroke pneumonia decreases the number of microglia, and promotes the activation of microglia 38

3.5. Post-stroke pneumonia increases the number of neutrophils in the blood, which is mitigated by amoxicillin treatment 41

3.6. Post-stroke pneumonia increases the number of infiltrating leukocytes in brain, whereas amoxicillin treatment did not show any significant effects 43

3.7. Post-stroke pneumonia significantly worsens neurological deficits in the subacute stroke phase, and also significantly impairs the performance of animals in the rotarod test until the chronic phase 44

3.8. Post-stroke pneumonia significantly increases brain atrophy and striatal atrophy in the chronic phase, and increases the reactivity of astrocytes 45

3.9. Neutrophil depletion alleviates the detrimental effects of post-stroke pneumonia 47

3.10. DNase I has no significant effect on stroke outcome, but increases brain hemorrhage formation 50

3.11. LDC7559 injection reduces the levels of NETs in blood, and reduces brain edema and IgG extravasation 53

4. DISCUSSION 57

5. CONCLUSION 62

6. SUMMARY 63

6.1. English summary 63

6.2. Deutsche Zusammenfassung 64

7. REFERENCES 65

8. ATTACHMENT 78

8.1. List of abbreviations 78

8.2. List of tables 79

8.3. List of figures 79

9. ACKNOWLEDGEMENTS 81

10. CURRICULUM VITAE 82

1. INTRODUCTION

1.1. Epidemiology of stroke

Stroke is one of the leading causes of long-term disability and the second leading cause of death, making it a significant global health burden (Feigin et al., 2021, Benjamin et al., 2019). Among all stroke patients, the majority suffer from ischemic stroke (62.4%), while the remaining cases are intracerebral hemorrhage (ICH) stroke (27.9%) and subarachnoid hemorrhage (SAH) stroke (9.7%) (Feigin et al., 2021). Stroke brings great economic burden to the society. Only in the U.S. in 2014 to 2015, the direct and indirect costs associated to stroke were estimated to be 45.5 billion dollars, and the total direct stroke-related costs are projected to be more than 94.3 billion dollars in 2035 (Benjamin et al., 2019).

1.2. Pathophysiology of ischemic stroke

The occlusion of a cerebral artery induces focal ischemia and infarct development. The cessation of blood supply elicits the neural cell death (Shi et al., 2019). Intracellular molecules named damage-associated molecular patterns (DAMPs) are released that initiate inflammatory responses via pattern recognition receptors (PRRs) (Endres et al., 2022). Microglia, resident immune cells in the brain, are the first to receive these signals, undergo morphological changes from ramified to amoeboid, and release cytokines and chemokines. Simultaneously, they begin to migrate towards the site of injury (Iadecola et al., 2020, Endres et al., 2022).

The local hypoglycemic and hypoxic state can also cause damage and death of vascular cells constituting the blood-brain barrier, leading to the disruption of the blood-brain barrier (Jiang et al., 2018). With the influence of DAMPs, cytokines, and chemokines, peripheral immune cells infiltrate the damaged brain tissue through the compromised blood-brain barrier (Bernardo-Castro et al., 2020, Jiang et al., 2018). These infiltrated immune cells can exacerbate the immune reaction and promote the

growth of the ischemic infarct into penumbral areas (Iadecola et al., 2020).

After the onset of ischemic stroke, the resident astrocytes in brain are stimulated by the inflammatory factors, and start to form the glial scar (Dzyubenko et al., 2018). This glial scar can limit inflammation and infection to the affected brain tissue (Bush et al., 1999, Dzyubenko et al., 2018). Along with the formation of scar tissue, immune cells with phagocytic functions, such as microglia, macrophages, and neutrophils, simultaneously engulf and clear the debris of dead cells, eventually establishing a stabilized stroke lesion (Neumann et al., 2009, Jia et al., 2021, Iadecola et al., 2020).

1.3. Current status and exploration of therapies for ischemic stroke

Tissue plasminogen activator (tPA) is a serine protease with thrombolytic function, which is the only drug approved by the U.S. Food and Drug Administration (FDA) for the treatment of ischemic stroke (Barthels and Das, 2020). A clinical trial published in 1995 revealed that compared to the placebo control group, patients treated with tPA were 30% more likely to be assessed as having minimal or no disability three months after a ischemic stroke (National Institute of Neurological Disorders and Stroke rt-PA Stroke Study Group, 1995). However, tPA treatment still has limitations, such as the narrow therapeutic time window, which is approximately 4.5 hours (Hacke et al., 2008). The application of tPA beyond the therapeutic time window may increase the risk of hemorrhagic transformation, leading to more severe consequences (Barthels and Das, 2020). Additionally, even in therapeutic time window, tPA application can also bring some risks like anaphylaxis and systemic bleeding (Barthels and Das, 2020, National Institute of Neurological Disorders and Stroke rt-PA Stroke Study Group, 1995).

In recent years, the clinical utilization of endovascular mechanical thrombectomy has been swiftly evolving. For ischemic stroke patients with large artery occlusion who do not respond well to tPA treatment, mechanical thrombectomy was shown to enhance stroke outcome (Evans et al., 2017). The therapeutic time window for mechanical thrombectomy is within 6 hours after the onset of ischemic stroke, longer than tPA's 4.5

hours (Evans et al., 2017). Moreover, some recent clinical trials have indicated that, when combined with standard medical therapy the time window for mechanical thrombectomy may be extended to 16 hours (Albers et al., 2018) or even 24 hours (Nogueira et al., 2018) after the occurrence of ischemic stroke. This therapeutic approach also faces some challenges, such as high requirements for patient eligibility (Jadhav et al., 2018), potentially resulting in severe complications like vessel perforation, symptomatic intracranial hemorrhage, subarachnoid hemorrhage, and arterial dissection (Ganesh and Goyal, 2018).

The ischemic core refers to the region where blood supply is reduced by more than 80% of baseline due to vascular occlusion. Cells within this area rapidly die due to severe ischemia, resulting in irreversible damage (Moskowitz et al., 2010). By contrast, the peripheral area of ischemia, known as penumbra, experiences a milder blood flow deficit. Neurons in this area stop functioning due to insufficient blood flow but remain alive (Lo, 2008, Iadecola et al., 2020). With time, neurons in the penumbra also die due to persistent insufficient blood flow, inflammatory responses, programmed cell death, and other reasons, thereby losing the therapeutic opportunity (Lo, 2008, Moskowitz et al., 2010). Researchers have made efforts in areas such as recanalization, reducing inflammation, inhibiting programmed cell death, and minimizing microthrombus formation. However, up to this point, the only successful clinical translations have been tPA and mechanical thrombectomy (Lu et al., 2019, Barthels and Das, 2020).

1.4. Stroke-associated pneumonia

A variety of complications, such as infections, gastrointestinal bleeding, myocardial infarction, deep vein thrombosis, and others, may occur after cerebral infarction (Kumar et al., 2010). Specifically, the incidence of infections can reach up to 30% (Westendorp et al., 2022). Among these infections, pneumonia and urinary tract infections are the most common (Westendorp et al., 2011). Particularly, pneumonia significantly escalates the unfavorable outcome and mortality of ischemic stroke patients (Chamorro et al.,

2012, Westendorp et al., 2022).

Currently, several factors are considered to be involved in the occurrence of stroke-associated pneumonia. Stroke-induced immunodepression is one of the factors (Westendorp et al., 2022). This stroke-induced immunodepression is thought to be associated with DAMPs and cytokines. After ischemic stroke onset, DAMPs and cytokines not only trigger local inflammatory responses but are also released into the peripheral circulation, resulting in transient immune system activation initially, followed by long-lasting immunodepression (Westendorp et al., 2022). Additionally, this immunodepression is also thought to be related to the activation of sympathetic nervous system (SNS), the parasympathetic nervous system (PNS), and the hypothalamus-pituitary-adrenal (HPA) axis (Liu et al., 2018). Lymphopenia and increased neutrophil-to-lymphocyte ratio are thought to be the main manifestations of stroke-induced immunodepression (Westendorp et al., 2022). Some researchers have begun exploring the use of neutrophil-to-lymphocyte ratio to predict the prognosis of ischemic stroke patients (Xu et al., 2023, Sharma et al., 2022). Presently, there is a perspective suggesting that the immunodepression serves as a protective mechanism of the body, to protect the brain from further inflammatory responses (Liu et al., 2018). However, it increases the risk of infections (Ghelani et al., 2021).

In addition, some studies have suggested that the brain-gut axis may also be involved in the development of post-stroke pneumonia (Li et al., 2023, Stanley et al., 2016). And some general risk factors, such as dysphagia, impaired consciousness, and mechanical ventilation are also thought to be related to the formation of pneumonia post stroke (Endres et al., 2022). It is important to note that in some patients with pneumonia post ischemic stroke, there are no causative infectious agents detected. This might be related to sterile lung injury, known as pneumonitis, which is caused by the inhalation of gastric acid. Alternatively, it could be due to anaerobic bacteria that require special culturing techniques (Kumar et al., 2010, Westendorp et al., 2011). Among the patients with bacterial pneumonia post stroke, the most commonly detected pathogens are

Streptococcus pneumoniae, *Klebsiella pneumoniae*, *Escherichia coli*, *Staphylococcus aureus*, *Pseudomonas aeruginosa*, and *Acinetobacter baumannii* (Westendorp et al., 2022).

At present, the main treatments for stroke-associated pneumonia are administering antibiotics and providing supportive care (Ghelani et al., 2021). However, antibiotics can affect the gut microbiota, which has been reported to potentially worsen the prognosis of ischemic stroke (Singh et al., 2016). Some clinical trials have attempted the prophylactic use of antibiotics to prevent the occurrence of stroke-associated pneumonia, however, these attempts have neither improved outcomes nor reduced the incidence of stroke-associated pneumonia (Endres et al., 2022, Westendorp et al., 2021). Furthermore, some investigations into the application of β-blockers and IFN-γ for the therapeutic and prophylactic management of stroke-associated pneumonia have been conducted, but all these explorations failed to show satisfactory results (Westendorp et al., 2022, Balla et al., 2021, Jagdmann et al., 2021).

It is widely recognized that stroke-associated pneumonia significantly worsens the prognosis of stroke patients (Endres et al., 2022). Most of the research to date concentrate on elucidating the mechanisms underlying the onset of stroke-associated pneumonia. Conversely, the exploration of mechanisms through which pneumonia influences the outcome of stroke patients is comparatively limited. A study suggested that the inflammatory response triggered by infection may elicit detrimental T helper cell type 1 (Th1) responses against cerebral antigens, including myelin basic protein and glial fibrillary acidic protein. These responses correlated with a decline in post-stroke functional outcomes and an expedited deterioration in cognitive abilities within the first year following stroke (Oh and Parikh, 2022, Becker et al., 2016). Additionally, a study indicated that the impact of stroke-associated pneumonia on stroke prognosis may be associated with interleukin 1 (IL-1) and platelet glycoprotein Iba (GPIbα) (Denes et al., 2014). Overall, the underlying mechanisms by which stroke-associated pneumonia impairs the prognosis of stroke remain unclear.

1.5. Role of neutrophils in ischemic stroke and pneumonia

As the most abundant leukocytes of the immune system, neutrophils play a vital role in the progression and recovery of ischemic stroke (Hermann and Gunzer, 2019). Neutrophils begin to infiltrate the infarcted brain tissue within a short time after a stroke occurs. Within 2 hours of the occurrence of a stroke, neutrophil rolling and adhesion begin to appear in the pial vessels (Kataoka et al., 2004, Hallenbeck et al., 1986). Neutrophils start to infiltrate into the brain tissue 6 to 8 hours after the onset of the ischemic stroke, and the infiltration reaches its peak at 24 to 48 hours (Jickling et al., 2015, Hallenbeck et al., 1986, Watcharotayangul et al., 2012). The accumulation of neutrophils in the brain can increase the infarct volume, exacerbate blood-brain barrier (BBB) disruption, and worsen the prognosis of ischemic stroke (Hermann and Gunzer, 2019, Jickling et al., 2015). Animal experiments have demonstrated that the depletion of neutrophils using lymphocyte antigen 6 complex locus G (Ly6G) antibodies can provide cerebral protection and improve neurological function recovery in animals after ischemic stroke (Yan et al., 2023, Neumann et al., 2015). Nevertheless, neutrophils are a crucial component of the human immune system. The clinical translation of neutrophil depletion strategies is impossible (Yan et al., 2023). Additionally, some animal experiments have found that injections of C-X-C motif chemokine receptor 2 (CXCR2) inhibitors, intercellular adhesion molecule 1 (ICAM-1) antibody, or very-late-antigen-4 (VLA-4) blockade can prevent neutrophils from infiltrating into brain tissue, thereby providing cerebral protection (Herz et al., 2015, Neumann et al., 2015, Zhang et al., 1995). However, clinical trials have shown that these methods cannot significantly improve the recovery of ischemic stroke patients (Hermann and Gunzer, 2019, Enlimomab Acute Stroke Trial, 2001).

Upon the occurrence of infection, neutrophils are rapidly released and migrate to the site of infection to engulf pathogens (Marsh et al., 1967, Liew and Kubes, 2019). Additionally, activated neutrophils can release DNA, histones, elastase, and other components to form a web-like structure known as neutrophil extracellular traps (NETs)

(Brinkmann et al., 2004). NETs have been reported to capture and kill pathogens, including bacteria, fungi, viruses, and parasites (Papayannopoulos, 2018). Furthermore, evidence from other animal studies suggest that the formation of NETs may contribute to the unfavorable outcomes of ischemic stroke, rendering NETs a potential target for ischemic stroke treatment (Denorme et al., 2022, Kang et al., 2020).

1.6. Aim of the study

Considering the high incidence rate of pneumonia among ischemic stroke patients and its detrimental impacts on the prognosis, it is particularly important to investigate the effects of pneumonia on the recovery of ischemic stroke and its underlying mechanisms, as well as to explore potential treatment strategies. In this study, we aimed to use middle cerebral artery occlusion (MCAO) mouse models to (1) evaluate the impact of experimentally induced *Streptococcus pneumoniae* pneumonia on ischemic injury and stroke recovery; (2) investigate the underlying mechanism of the effects; and (3) explore treatments to improve stroke outcome.

2. MATERIALS AND METHODS

2.1. Legal issues, animal housing, randomization and blinding

All procedures were conducted with the consent of responsible local authorities (Bezirksregierung Düsseldorf) and complied with EU regulations (Directive 2010/63/EU) regarding the care and use of laboratory animals. Results were reported in accordance to Animal Research: Reporting of In Vivo Experiments (ARRIVE) guidelines. Experiments were strictly randomized. Throughout the study, the researcher conducting the animal experiments, behavioral assessments, and histochemical analyses was completely blinded at every stage by another researcher who prepared the injectable solutions. These solutions with dummy names (A and B) were unblinded after termination of the study. Mice were kept in a regularly inversed 12-hour light/ 12-hour dark cycle in groups of 5 animals/ cage. All mice had free access to food and drinking water. Behavioral tests and animal surgeries were always performed in the morning hours throughout the study.

2.2. Focal cerebral ischemia

MCAO mouse models were induced as described before (Yin et al., 2023). Using an animal anesthesia apparatus (**Figure 1A**), 10~12 weeks old male C57BL6/j mice (Envigo, Darmstadt, Germany) were anesthetized by a gas mixture consisting of 1.5% isoflurane, 30% oxygen, with the remainder being nitrous oxide. 150 µl of buprenorphine (0.1 mg/kg) was injected subcutaneously for analgesia. During the surgery, the rectal temperature was monitored and kept at 37°C using a feedback-controlled heating system (**Figure 1B**). A surgical microscope (**Figure 1C**) was utilized for surgical field inspection. A flexible probe was attached to the skull of the animal, positioned over the central area of the middle cerebral artery territory, to record the cerebral blood flow by laser Doppler flowmetry (LDF) monitoring system (**Figure 1D**). Following the execution of a midline cervical incision, the left common

carotid artery (CCA), internal carotid artery (ICA), and external carotid artery (ECA) were subsequently exposed (**Figure 1E**). The CCA and ECA were ligated by sutures, while the ICA was subjected to temporary clipping. A silicone-coated 7.0 nylon monofilament was inserted into the CCA via a minor incision and pushed forward through ICA to the division of the middle cerebral artery (**Figure 1F**). Blood flow was halted for 30 minutes, after which the filament was removed to start reperfusion. The incisions were carefully stitched. For the initial 3 days following the stroke, the animals were administered daily intraperitoneal injections of carprofen (4 mg/kg). All equipment and materials used in surgery are listed in **Table 1**.

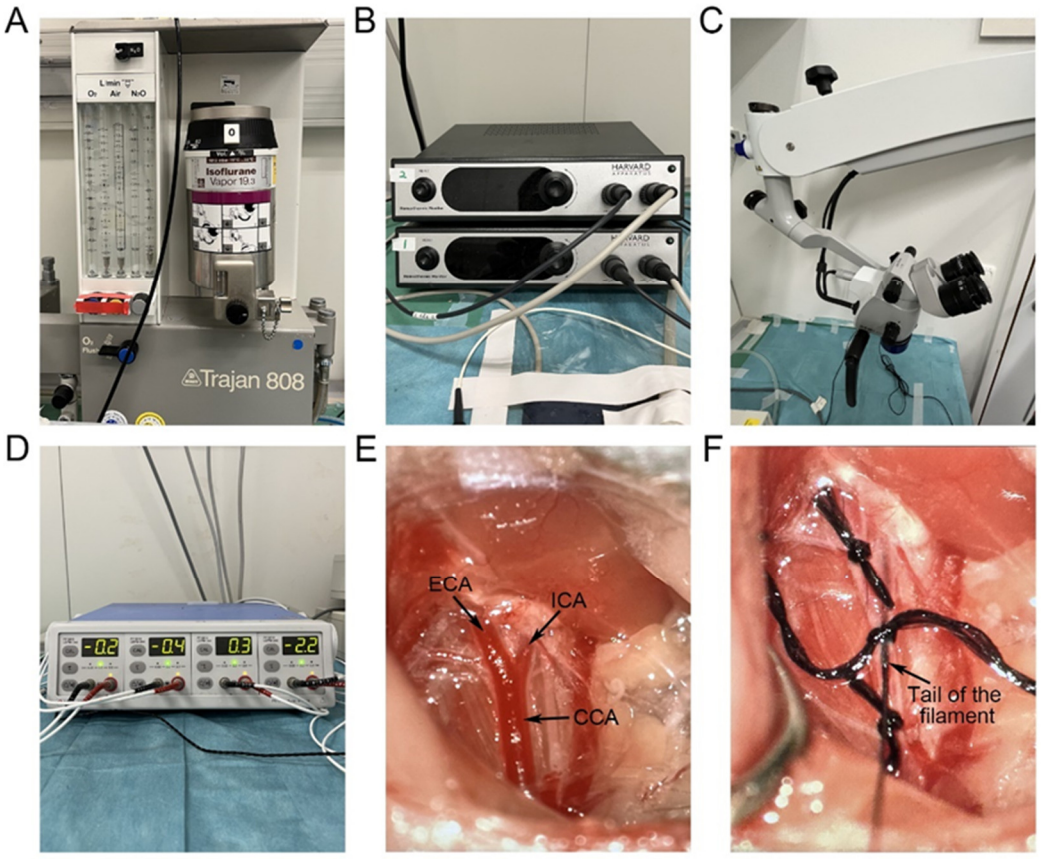

Figure 1. Main surgery instruments and surgical fields

(A) Animal anesthesia apparatus. (B) Feedback-controlled heating system. (C) Surgical microscope. (D) LDF monitoring system. (E) Exposure of CCA, ECE and ICA in surgery. (F) Monofilament was inserted and pushed into CCA.

Table 1. Equipment and materials used in surgery

Equipment and materials	Manufacturer
Animal anesthesia apparatus	Dräger Trajan 808, QMS Medical Technology, Germany
Feedback-controlled heating system	Fluovac, Harvard Apparatus, Holliston, MA, U.S.A.
Surgical microscope	Carl Zeiss, Oberkochen, Germany
LDF monitoring system	Perimed Instruments, Rommerskirchen, Germany
Silicon-coated monofilament (Cat# 702234PK5Re)	Doccol, Sharon, MA, USA
Isoflurane	Piramal Critical Care, Hallbergmoos, Germany
Buprenorphine	Reckitt Benckiser, Slough, U.K.
Carprofen	Bayer Vital, Leverkusen, Germany
Silk suture 5-0 (Cat# K890H)	Ethicon, Norderstedt, Germany
Silk suture 7-0 (Cat# EH7464G)	Ethicon, Norderstedt, Germany
Spring scissors (Cat# 15024-10)	Fine Science Tools, Heidelberg, Germany
Standard scissors (Cat# 14568-12)	Fine Science Tools, Heidelberg, Germany
Vannas spring scissors (Cat# 15000-00)	Fine Science Tools, Heidelberg, Germany
Halsey micro needle holder (Cat# 12500-12)	Fine Science Tools, Heidelberg, Germany

2.3. Animal allocation

After MCAO surgery, animals were randomly assigned to the following experimental groups. Numbers of animals in each group can be found in **Table 2**.

Table 2. Animal allocation

Animal set	Group	Number
Set 1 (2 dpp)	Vehicle	7
	Amoxicillin	7
	Pneumonia/ vehicle	7
	Pneumonia/ Amoxicillin	7
Set 2 (Flow cytometry)	Vehicle	8
	Amoxicillin	8
	Pneumonia/ vehicle	7
	Pneumonia/ Amoxicillin	8
Set 3 (7 dpp)	Vehicle	8
	Amoxicillin	9
	Pneumonia/ vehicle	8
	Pneumonia/ Amoxicillin	9
Set 4 (14 days)	Vehicle	8
	Amoxicillin	8
	Pneumonia/ vehicle	8
	Pneumonia/ Amoxicillin	8
Set 5 (56 dpp)	Vehicle	12
	Amoxicillin	12
	Pneumonia/ vehicle	11
	Pneumonia/ Amoxicillin	12
Set 6 (Neutrophil depletion)	Isotype	6
	Ly6G antibody	7
	Pneumonia/ Isotype	7
	Pneumonia/ Ly6G antibody	7

Set 7 (DNase I)	Vehicle	6
	DNase I	8
	Pneumonia/ Vehicle	6
	Pneumonia/ DNase I	7
Set 8 (LDC7559)	Vehicle	10
	LDC7559	8
	Pneumonia/ Vehicle	7
	Pneumonia/ LDC7559	8
Total		259

2.4. *Streptococcus pneumoniae* culture and pneumonia induction

The cultivation of bacteria and induction of pneumonia have previously been described (Zec et al., 2023). For the lung infection, a strain of pneumococcal serotype 1 (*S. pneumoniae* SV1, ATCC 33400) was employed. *S. pneumoniae* were incubated at 37°C overnight on Columbia blood agar plates (Oxoid, PB5039A). Individual colonies were then picked and propagated in 10 ml of Brain–Heart Infusion Broth (Thermo Fisher Scientific, Im Steingrund 4-6, 63303 Dreieich, Germany), until they reached the mid-logarithmic phase of growth (OD600 = 0.045–0.055; measured with NanoDrop 1000). After reaching the desired growth phase, 800 µl of the bacterial culture was mixed with 200 µl of 86% glycerol and stored at −80°C for future use. To prepare for the actual infection, *S. pneumoniae* were cultured again to the mid-logarithmic phase, then collected by centrifugation at 1,500g for 10 minutes at 4°C. The collected bacterial pellet was then resuspended in 550 µl of phosphate-buffered saline (PBS). For the infection procedure, 50 µl of the bacterial suspension, containing approximately 1 x 10^8 colony-forming units (CFUs) of *S. pneumoniae*, was administered per animal.

3 days post stroke, the animals were subjected to pneumonia induction. Initially, anesthesia was administered through an intraperitoneal injection, consisting of 80 mg/kg of ketamine and 10 mg/kg of xylazine. Subsequently, the mouse was positioned at a

60-degree angle on a self-made stand and secured with Velcro straps. A small rubber band was employed to hold the mouse's teeth in place, while gently pulling out the tongue. A 22-gauge, blunt-ended cannula was then carefully inserted into the trachea of the mouse, aided by a specialized small-animal laryngoscope (73-4867, Harvard Apparatus, Holliston, MA, U.S.A.). After the needle's removal, a volume of 50 µl of the bacterial suspension was administered into the cannula using a pipette. To ensure the liquid was evenly distributed throughout the lungs and to assist in breathing, the MiniVent 845 (73-4867, Harvard Apparatus) ventilator was connected to the cannula.

2.5. Drug administration

Three hours following the induction of pneumonia, the animals received a subcutaneous (s.c.) injection of the antibiotic amoxicillin (15 mg/kg; Duphamox LA; Zoetis, Berlin, Germany) or an equivalent volume of vehicle (Lipovenös MCT 20%; Fresenius Kabi, Bad Homburg, Germany). This injection process was carried out every 8 hours until the third day post-pneumonia (dpp), in a total of nine injections (Abgueguen et al., 2007).

For neutrophil depletion, an intraperitoneal (i.p.) injection of 200 µg of anti-Ly6G antibody (clone 1A8; BioXCell, West Lebanon, NH, USA) or a control IgG (clone 2A3; BioXCell) was administered 24 hours before the induction of pneumonia and again 24 hours following the induction of pneumonia (Wang et al., 2020).

To degrade circulating DNA, Deoxyribonuclease I (DNase I; 11284932001; Roche, Basel, Switzerland) was administered through an intravenous (i.v.) injection at a dosage of 10 µg and through an i.p. injection at a dosage of 50 µg 30 minutes before inducing pneumonia. The i.p. injection was then repeated at 12-hour intervals until the time of animal euthanasia. For control treatment, a comparable volume of vehicle was administered following the same protocol (Kang et al., 2020).

To inhibit the formation of NETs, the gasdermin D inhibitor LDC7559 (10mg/kg; HY-111674; MedChemExpress, Monmouth Junction, NJ, U.S.A.) was dissolved in DMSO for stock, and then further diluted in corn oil for injection. It was i.p. injected

(10 mg/kg) about 30 minutes prior to pneumonia. An equivalent volume of vehicle was injected using the same method for the control group (Tuz et al., 2024).

2.6. Neurological deficit score

Neurological deficits were blindly assessed blindly by modified Clark score, which contains two parts, general deficits and focal deficits (Clark et al., 1997). The total score ranges from 0 (healthy) to 39 (the worst) (**Table 3**). Assessments were conducted daily up to 7 dpp, then on days 9, 11, and 14, followed by weekly assessments until 56 dpp.

Table 3. Modified Clark score

General deficits (total score 0-13)	
1. Hair (score 0-2)	
Mouse observed on open bench top. Observation with no interference.	
1.1. Hair neat and clean.	0
1.2. Lack of grooming, piloerection and dirt on the fur around nose and eyes.	1
1.3. Lack of grooming, piloerection and dirty coat, extending beyond just nose and eyes.	2
2. Eyes (score 0-4)	
Mouse observed on open bench top. Observation with no interference or stimulation.	
2.1. Open and clear (no discharge).	0
2.2. Open and characterized by milky white mucus.	1
2.3. Open and characterized by milky dark mucus.	2
2.4. Eyes clotted (one or both sides).	3
2.5. Closed.	4
3. Posture (score 0-4)	
Place the mouse on the palm of your hand and rock gently to observe stability.	

3.1. The mouse stands in the upright position on four limbs with the back parallel to the palm. During the rocking movement, it uses its limbs to stabilize itself.	0
3.2. The mouse stands humpbacked. During the rocking movement, it lowers its body instead of using its limbs to gain stability	1
3.3. The head or part of the trunk lies on the palm.	2
3.4. The mouse reclines to one side but may be able to turn to an upright position with some difficulty.	3
3.5. No upright position possible.	4

4. Spontaneous activity (score 0-3; duration 1 minute)

Mouse observed on open bench top. Observation with no interference or stimulation.

4.1. The mouse is alert and explores actively.	0
4.2. The mouse seems alert, but it is calm and quiet and it starts and stops exploring repeatedly and slow.	1
4.3. The mouse is listless, moves sluggishly but does not explore.	2
4.4. The mouse is lethargic or stuporous and barely moves during the 1 minute.	3

Focal deficits (total score 0-26)

5. Body symmetry (score 0-2)

Mouse observed on open bench top. Observation of undisturbed resting behavior and description of the virtual nose-tail line.

5.1. Normal. a, Body: normal posture, trunk elevated from the bench, with forelimbs and hindlimbs leaning beneath the body; b, Tail: straight.	0
5.2. Slight asymmetry. a, Body: leans on one side with forelimbs and hindlimbs leaning beneath the body; b, Tail: slightly bent.	1
5.3. Moderate asymmetry. a, Body: lean on one side with forelimbs and hindlimbs stretched out; b, Tail: slightly bent.	2

6. Gait (score 0-4)

Mouse observed on open bench top. Observation of undisturbed movements.

6.1. Normal. Gait is flexible, symmetric, and quick.	0
6.2. Stiff, inflexible. The mouse walks humpbacked, slower than normal mouse.	1
6.3. Limping with asymmetric movements.	2
6.4. More severe limping, drifting, falling with obvious deficiency in gait.	3
6.5. Does not walk spontaneously. (In this case, stimulation will be performed gently pushing the mouse with a pen. When stimulated, the mouse walks no longer than three steps).	4

7. Climbing (score 0-3)

Mouse is placed in the center of a gripping surface at an angle of 45°.

7.1. Normal. The mouse climbs quickly.	0
7.2. Climbs slowly, limb weakness present.	1
7.3. Holds onto slope, does not slip or climb.	2
7.4. Slides down slope, unsuccessful effort to prevent fall.	3

8. Circling behavior (score 0-3)

Mouse observed on open bench top. Observation of undisturbed movements.

8.1. Circling behavior absent. The mouse turns equally to left or right.	0
8.2. Predominantly one-sided turns. Optional: record to which side the mouse turns.	1
8.3. Circles to one side, although not constantly.	2
8.4. Circles constantly to one side. This one is now highlighted in yellow.	3

9. Forelimb symmetry (score 0-4)

Mouse suspended by the tail. Movements and position of forelimbs are observed.

9.1. Normal. Both forelimbs are extended towards the bench and move actively.	0
9.2. Light asymmetry. Contralateral forelimb does not extend entirely.	1

9.3. Marked asymmetry. Contralateral forelimb bends towards the trunk. The body slightly bends on the side ipsilateral to the stroke. 2

9.4. Prominent asymmetry. Contralateral forelimb adheres to the trunk. 3

9.5. Slight asymmetry, no body/limb movement. 4

10. Compulsory circling (score 0-3)

Forelimbs on bench, hindlimbs suspended by tail. This position reveals the presence of the contralateral limb palsy. In this handstand position, limb weakness is displayed by a circling behavior when the animal attempts forward motion.

10.1. Absent. Normal extension of both forelimbs. 0

10.2. Both forelimbs extended but begins to circle predominantly to one side. 1

10.3. Circles only to one side and may fall to one side. 2

10.4. Pivots to one side sluggishly and does not rotate in a full circle. Mouse will fall to one side. 3

11. Whisker response (score 0-4)

Mouse is placed on the bench. Using a pen, touch the whiskers and the tip of ears gently from behind, first on the lesioned side and then on the contralateral side.

11.1. Normal symmetrical response. The mouse turns the head towards the stimulated side and withdraws from the stimulus. 0

11.2. Light asymmetry. The mouse withdraws slowly when stimulated on the paretic side. Normal response on the side ipsilateral to the stroke. 1

11.3. Prominent asymmetry. No response when stimulated on the paretic side. Normal response on the side ipsilateral to the stroke. 2

11.4. Absent response on the paretic side, slow response when stimulated on the side ipsilateral to the stroke. 3

11.5. Absent response bilaterally. 4

12. Gripping test of the forepaws (score 0-3)

Mouse is held by the tail on the wire bar cage lid, so that the forepaws touch the

grid.	
12.1. Mouse grasps the grid firmly with forepaws and tries to place the hind paws also onto the grid by pulling the hind paws under the body.	0
12.2. Mouse accesses the grid but has less power. A slight pull breaks the grip of the forepaws.	1
12.3. Mouse cannot grip with the impaired forepaw.	2
12.4. Mouse cannot grip the grip.	3

2.7. Behavioral tests

We conducted two behavioral tests, the tight rope and rotarod tests. The tight rope test consists of a 60-cm-long rope connected to two platforms. Animals are positioned at the rope's midpoint, and the time until dropping off or until they reach a platform is recorded, with a maximum of 60 seconds for the test period. Prior to the study, animals underwent trainings 3 times daily for 3 days. Following baseline evaluation, the mice were subjected to the test on 0 dpp before the pneumonia induction, with subsequent weekly assessments until 56 dpp (Mohamud Yusuf et al., 2022). The translation of the time results into a quantitative score is detailed in **Table 4** (Doeppner et al., 2011).

The rotarod is a motor-coordination test that is assessed on a rotating drum (Ugo Basile, model 47600, Comerio, Italy). Mice were positioned on the drum, which then began to accelerate from 4 rpm to 40 rpm. The time when the animal dropped off the drum was recorded with a maximum of 300 seconds for each testing session. The animals were trained 3 times a day for 3 days before the experiments. After a baseline assessment, the mice were evaluated from 0 dpp prior to the induction of pneumonia, followed by weekly assessments up to 56 dpp (Mohamud Yusuf et al., 2022).

Table 4. Scoring of tight rope test performance

Score	Time (second)	Platform arrival
20	1-6	+
19	7-12	+
18	13-18	+
17	19-24	+
16	25-30	+
15	31-36	+
14	37-42	+
13	43-48	+
12	49-54	+
11	55-60	+
10	55-60	-
9	49-54	-
8	43-48	-
7	37-42	-
6	31-36	-
5	25-30	-
4	19-24	-
3	13-18	-
2	7-12	-
1	1-6	-
0	0	-

2.8. Measurement of infarct volume, brain edema, brain atrophy and brain hemorrhage

Under deep isoflurane anesthesia, mice were transcardially perfused with cold 0.01 M PBS followed by 4% paraformaldehyde (PFA; 8187151000; Millipore, Darmstadt, Germany) in 0.01 M PBS. Following animal sacrifice, brain tissues were harvested and fixed in 4% PFA solution for 24 hours. Subsequently, the tissues underwent dehydration through 15% and 30% sucrose solutions (S9378; Sigma-Aldrich, St. Louis, MO, U.S.A.) at 4°C until they sank to the bottom. Before being preserved at -80°C for future use, the samples were immersed in dry ice-precooled isopentane (143501; AppliChem, Darmstadt, Germany). Coronal sections with a thickness of 20 μm were prepared on a cryostat (CM 1950; Leica, Wetzlar, Germany) at intervals of 1 mm for future staining.

Cresyl violet staining was employed to evaluate infarct volume, brain edema, and brain atrophy. Sections were scanned and analyzed by ImageJ software (National Institute of Health, Bethesda, MD, U.S.A.). For animals sacrificed 2 dpp, the volume of the infarct was calculated by subtracting the volume of the healthy tissue in the ischemic hemisphere from the volume of tissue in the contralateral hemisphere. Brain edema was assessed by evaluating the proportion of the increased volume in the ipsilateral side relative to the contralateral side. For the analysis of brain hemorrhages, slices at the bregma level underwent incubation in a 0.05% diaminobenzidine (DAB) solution (D5905; Sigma-Aldrich) for 2 minutes. This compound, when oxidized by the peroxidases of red blood cells, produced a dark brown staining. The frequency and size of the brain hemorrhages were then evaluated (Yin et al., 2023).

In animals sacrificed at 7, 14, and 56 dpp, atrophy was evaluated by the volume reduction of the ipsilateral striatum or hemisphere relative to the contralateral striatum or hemisphere (Yin et al., 2023).

2.9. Immunohistochemistry

Tissue sections were incubated at room temperature for 30 minutes in 0.01 M PBS

containing 0.1% Triton X-100, followed by a rinse with 0.01 M PBS. Subsequently, the sections were incubated at room temperature for 1 hour in 0.01 M PBS containing 10% normal donkey serum. After this incubation, the sections were incubated overnight at 4°C in primary antibodies. The primary antibodies used included monoclonal rabbit anti-neuronal nuclear antigen (NeuN), monoclonal rat anti-cluster of differentiation-45 (CD45), polyclonal goat anti-intercellular adhesion molecule-1 (ICAM-1), monoclonal rat anti-glial fibrillary acidic protein (GFAP), polyclonal rabbit anti-collagen type IV (collagen IV), monoclonal rat anti-glycoprotein Ibα (GPIbα), and polyclonal rabbit anti-ionized calcium binding adaptor molecule 1 (Iba-1). Following a 0.01 M PBS wash, the tissue was incubated at room temperature for 1 hour with appropriate secondary antibodies and fluorescent DNA dyes (Hoechst 33342). After rinsing, the sections were mounted with a mounting medium, and then scanned by microscope. Detailed information of the antibodies and reagents used are listed in **Table 5**.

Table 5. Antibodies and reagents used in immunohistochemistry

Antibodies and reagents	**Manufacturer**
Monoclonal rabbit anti-NeuN (ab177487)	Abcam, Cambridge, UK
Monoclonal rat anti-CD45 (05-1416)	Merck Millipore, Darmstadt, Germany
Polyclonal goat anti-ICAM-1 (AF796)	R&D, Minneapolis, MN, USA
Monoclonal rat anti-GFAP (13-0300)	Thermo Fisher Scientific, Waltham, MA, USA
Polyclonal rabbit anti-collagen IV (AB756P)	Merck Millipore, Darmstadt, Germany
Monoclonal rat anti-GPIbα (M043-0)	Emfret Analytics, Eibelstadt, Germany
Polyclonal rabbit anti-Iba-1 (019-19741)	Wako, Osaka, Japan
Hoechst 33342 (62249)	Thermo Fisher Scientific, Waltham, MA, USA

Immun-mount (9990402)	Epredia, Portsmouth, NH, USA
Donkey anti-rat IgG secondary antibody Alexa Fluor 594 (A21209)	Thermo Fisher Scientific, Waltham, MA, USA
Donkey anti-rabbit IgG secondary antibody alexa Fluor 594 (A21207)	Thermo Fisher Scientific, Waltham, MA, USA
Donkey anti-goat IgG secondary antibody Alexa Fluor 594 (A11058)	Thermo Fisher Scientific, Waltham, MA, USA
Donkey anti-mouse IgG secondary antibody Alexa Fluor 594 (A21203)	Thermo Fisher Scientific, Waltham, MA, USA
Donkey anti-rabbit IgG secondary antibody alexa Fluor 488 (A21206)	Thermo Fisher Scientific, Waltham, MA, USA
Donkey anti-rat IgG secondary antibody alexa Fluor 488 (A21208)	Thermo Fisher Scientific, Waltham, MA, USA
Triton X-100 (648462)	Sigma-Aldrich, St. Louis, MO, USA
Normal donkey serum (D9663)	Sigma-Aldrich, St. Louis, MO, USA

Immunofluorescence stainings were scanned using an inverted microscope (Axio Observer.Z1; Carl Zeiss, Oberkochen, Germany). The obtained images were analyzed using ImageJ software. Extravasated IgG, ICAM-1, and GFAP were evaluated by integrated signal intensities. To analyze microglia/ macrophage (Iba-1) and infiltrated $CD45^+$ cells, six 300 µm × 300 µm ROIs were chosen to calculate density. To assess the microthrombosis, the density of vessels with microclots (collagen-IV/GP-Ibα) in ipsilateral hemisphere was calculated. To evaluate neuronal survival within the ipsilateral striatum, density was calculated on three 300 µm × 300 µm ROIs. The calculated density values were subsequently multiplied by the total area covered by surviving neurons in the ipsilateral striatum to estimate their overall number.

2.10. Microglia/macrophage morphology analysis

For the analysis of microglia/ macrophage morphology, the Iba-1 immunofluorescence staining procedure was used as described above. Images were obtained from both the border and core of the infarct using a Leica SP8 confocal microscope (objective: HC PL APO CS2 63x/1.30, Leica Microsystems, Wetzlar, Germany). Z-stacks with dimensions of 184.52×184.52×15 µm were acquired with an interslice distance of 0.5 µm. The 3D morphology of cells was analyzed using MATLAB (MathWorks, Natick, MA, U.S.A.) based program 3DMorph following previously outlined methods. Briefly, cells were identified through automated thresholding and segmentation processes. Morphological characteristics including cell territory, volume, and ramification index (ramification index = territory / volume) were calculated following skeletonization of the cells (York et al., 2018).

2.11. Flow cytometry

Flow cytometry was done by previously described (Yin et al., 2023). Blood samples were obtained from the animals' hearts prior to sacrifice at 2 dpp. And ischemic brain hemispheres were collected from the same animals after the perfusion with cold 0.01M PBS for further use. For blood sampling, after incubation with erythrocyte lysis buffer (BD Biosciences, New Jersey, USA) for 7 min and exposure to two washing steps by cold 0.01M PBS, single-cell suspensions were obtained. Brain tissue samples underwent mechanical disaggregation using a 70 µm cell strainer (Life Sciences, New York, NY, USA) placed over a culture dish, followed by a centrifugation with 37% Percoll solution (GE Healthcare, Uppsala, Sweden). The sediment obtained was then subjected to washing steps, from which cell suspensions were harvested. These single-cell suspensions were then stained with antibody cocktails (listed in **Table 6)** for 30 minutes at 4 °C. Following this, cell suspensions were analyzed using a Cytoflex flow cytometer (Beckman–Coulter, Brea, CA, U.S.A.) and FlowJo software V10 (Ashland, OR, U.S.A.). The gating strategy is detailed in **Figure 2**.

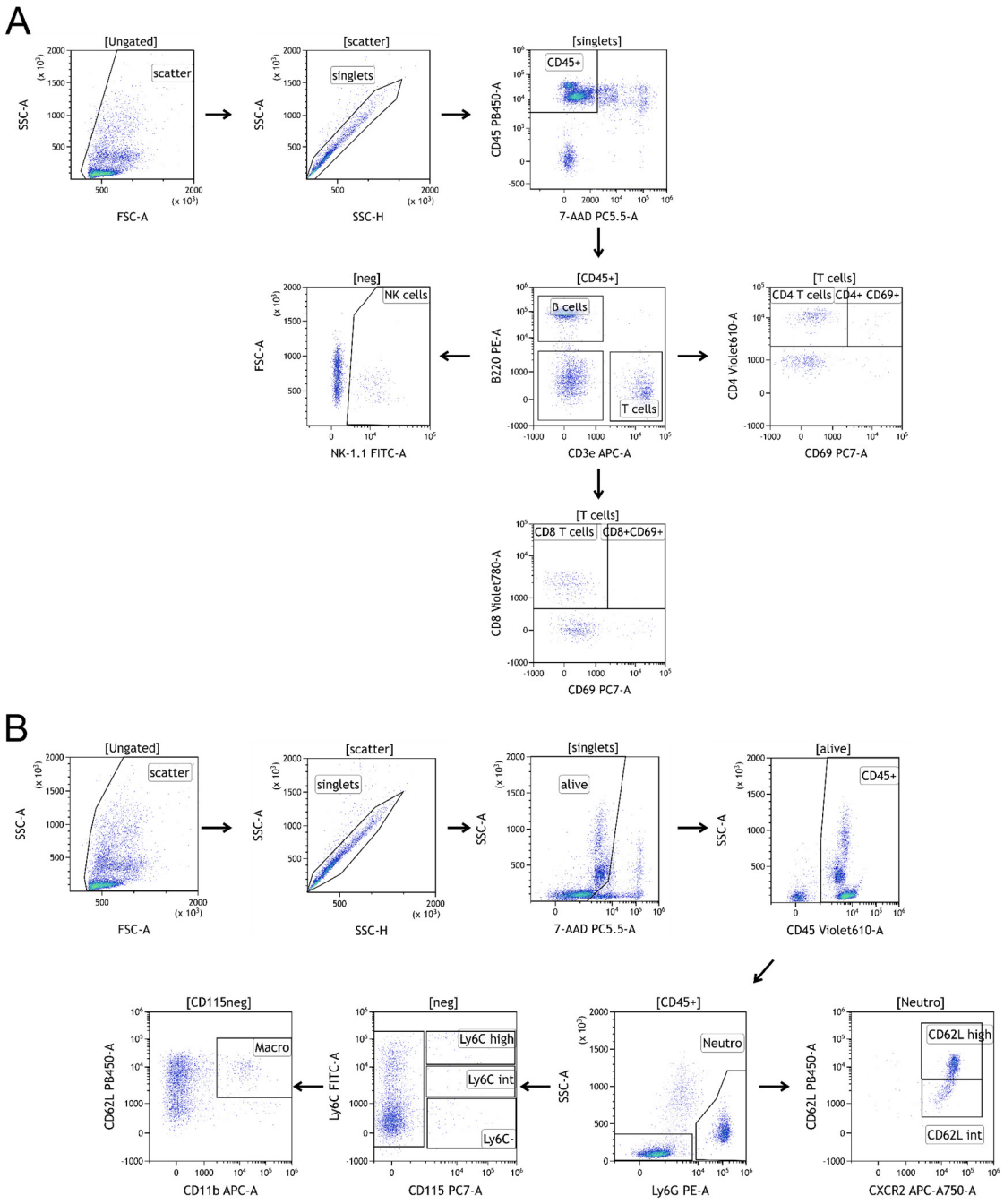

Figure 2. Flow cytometry gating strategies.

Gating strategies used for analyzing brain and peripheral blood leukocytes and leukocyte activation via flow cytometry. (A) Lymphoid and (B) myeloid cells were examined separately.

Table 6. Flow cytometry antibody panel

Antigen	Conjugate	Host/isotype	Clone	Supplier
Mouse CD45	Pacific blue	Rat IgG2b, kappa	30F11	BioLegend
Mouse CD45	BV 605	Rat IgG2b, kappa	30F11	BioLegend
Mouse Ly6G	Phycoerythrin (PE)	Rat IgG2a, kappa	1A8	BioLegend
Mouse CXCR2 (CD182)	APC/Cyanine7	Rat IgG2a, kappa	SA044G4	BioLegend
Mouse CD62L	eFluor 450	Rat IgG2a, kappa	MEL-14	eBioscience
Mouse Ly6C	Fluorescein isothiocyanate (FITC)	Rat IgM, kappa	AL21	BD Biosciences
Mouse CD11b	Allophycocyanin (APC)	Rat IgG2b, kappa	M1/70	eBioscience
Mouse CD115	PE-Cy7	Rat IgG2a, kappa	AFS98	eBioscience
Mouse CD3ε	Alexa Fluor 647	Hamster IgG	145-2C11	BioLegend
Mouse CD4	BV 605	Rat IgG2a, kappa	RM4-5	BD Biosciences
Mouse CD8	BV 786	Rat IgG2a, kappa	53-6.7	BD Biosciences
Mouse B220	PE	Rat IgG2a, kappa	RA3-6B2	BD Biosciences
Mouse NK-1.1	FITC	Rat IgG2a, kappa	PK136	BD Biosciences
Mouse CD69	PE-Cy7	Hamster IgG	H1.2F3	BioLegend

2.12. Quantification of NETs in mouse plasma samples

At 2 dpp, blood samples were obtained from the animals' hearts in deep anesthesia before sacrifice. Then, the blood samples were centrifuged at 4°C, first at 3,000 g for 10 minutes and subsequently at 8,000 g for 10 minutes. The plasma samples obtained were stored at -80°C for future use. NET levels in plasma were determined using a capture ELISA (Cell Death ELISA^{PLUS}, 11774425001, Roche, Basel, Switzerland) for

measuring citrullinated histone H3 (CitH3) that was associated with DNA. Anti- CitH3 antibody (5 µg/ml; ab5103, Abcam, Cambridge, U.K.) was applied to 96-well plates in a volume of 50 µl for overnight coating at 4°C. This procedure was followed by antigen blocking with 5% BSA for 2 hours at 300 rpm on a shaker. After blocking, the wells were washed three times with 300 µl of washing buffer. Subsequently, 50 µl of plasma and 80 µl of incubation buffer containing peroxidase-conjugated anti-DNA antibody were added and incubated for 2 hours at 300 rpm. Then, the wells were washed three times with 300 µl incubation buffer. After that, 100 µl of peroxidase substrate was added to each well, and the plates were incubated for 30 minutes in the dark at room temperature at 300 rpm. The reaction was halted by adding 100 µl of ABTS peroxidase stop solution to each well. Absorbance was measured at 405 nm and was subtracted by absorbance at 490 nm (absorbance at 405 nm minus absorbance at 490 nm). The absorbance values were directly correlated with the concentrations of soluble NETs and were displayed as a relative elevation compared to the control (Tuz et al., 2024).

2.13. Statistical data analysis

Statistical analyses were conducted using GraphPad Prism version 9.5.1 for Windows (GraphPad Software, San Diego, California, USA). LDF recordings, neurological deficits, and behavioral tests underwent analysis through repeated measurement ANOVA with subsequent LSD posthoc tests. Data were presented as mean ± standard deviation (SD). For histochemical staining data that were normally distributed, one-way analysis of variance (ANOVA) was utilized, followed by LSD posthoc test. For data that did not follow a normal distribution, the Kruskal-Wallis test followed by Dunn's tests was employed. This part of data is presented in box plots with median and mean ± interquartile ranges (IQR) with minimum and maximum data as whiskers. Hemorrhage incidence data were assessed by Fisher's exact test and reported as percentage rates. P values < 0.05 were considered to statistical significance.

3. RESULTS

3.1. Post-stroke pneumonia exacerbates neurological deficits, brain edema, and IgG extravasation in the acute stroke phase

First, we evaluated the impact of post-stroke pneumonia on neurological deficits and ischemic injury at 2 dpp and studied the effect of the antibiotic amoxicillin on stroke severity. LDF recordings showed that there were no significant differences between the groups during the MCAO and reperfusion, indicating that our ischemic stroke model was reproducible (**Figure 3A**). On the first two days after pneumonia, the neurological deficits were significantly aggravated by pneumonia (**Figure 3B**). Although pneumonia did not affect the infarct volume (**Figure 3C**), it significantly exacerbated brain edema (**Figure 3D**) and IgG extravasation (**Figure 3E**), both of which reflect the aggravation of blood-brain barrier damage. Although amoxicillin treatment did not show significant therapeutic effects on neurological deficits (**Figure 3B)**, brain edema (**Figure 3D**), and IgG extravasation (**Figure 3E**), there was a tendency toward alleviation in the antibiotic studies.

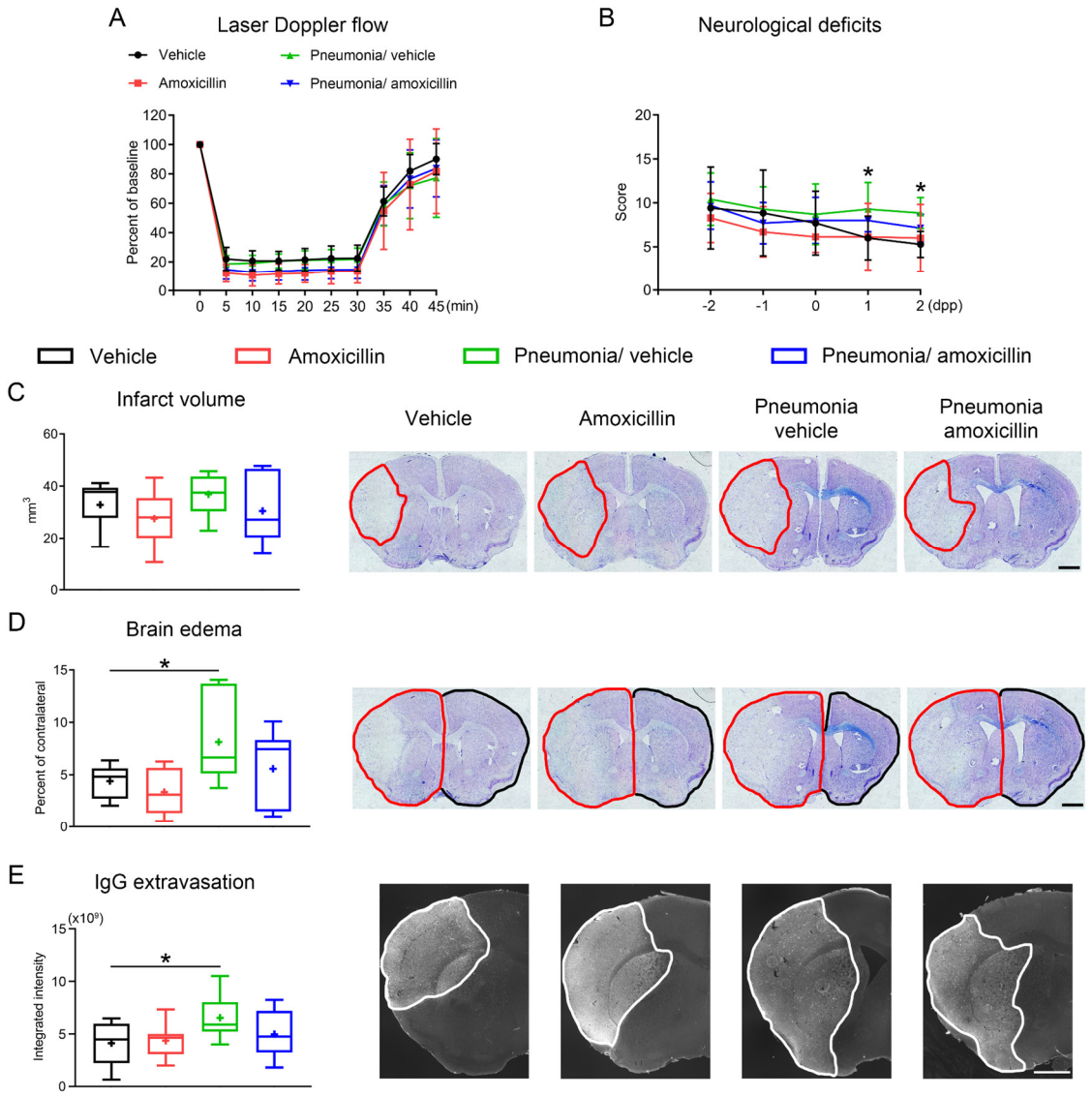

Figure 3. At 2 dpp, the effects of pneumonia on neurological deficits, brain edema, and IgG extravasation, and the therapeutic efficacy of amoxicillin.

(A) LDF records during occlusion and reperfusion, **(B)** neurological deficits assessed by the Clark score, **(C)** infarct volume and **(D)** brain edema evaluated by cresyl violet staining, and **(E)** IgG extravasation staining assessed at 2 dpp in mice that exposed to 30 minutes of MCAO. The representative cresyl violet staining and IgG extravasation staining are shown. Scale bars in **(C)**, **(D)** and **(E)** are 1 mm. Asterisks in **(B)** indicate the comparison between vehicle group and pneumonia/ vehicle group. *$p<0.05$ (n=7 animals/group).

3.2. Post-stroke pneumonia aggravates peripheral leukocyte infiltration and microvascular ICAM-1 expression

Upon observing the effects of post-stroke pneumonia on neurological deficits and ischemic injury, we proceeded to investigate the implications of pneumonia at the cellular level. From immunofluorescence staining, pneumonia did not induce significant differences in neuronal survival (**Figure 4A**) or astrocyte immunoreactivity (**Figure 4B**). However, pneumonia induced after stroke significantly increased the infiltration of peripheral immune cells in the brain (**Figure 4C**). Additionally, it also increased the abundance of ICAM-1 (**Figure 4D**), an adhesion molecule that can participate in mediating the migration and infiltration of leukocytes on brain microvessels. Increased leukocyte infiltration and upregulation of ICAM-1 expression may contribute to more severe neurological deficits, brain edema, and IgG extravasation. Importantly, amoxicillin treatment did not show significant effects on neuron survival, astrocyte immunoreactivity, leukocyte infiltration, and ICAM-1 expression (**Figure 4A-D**).

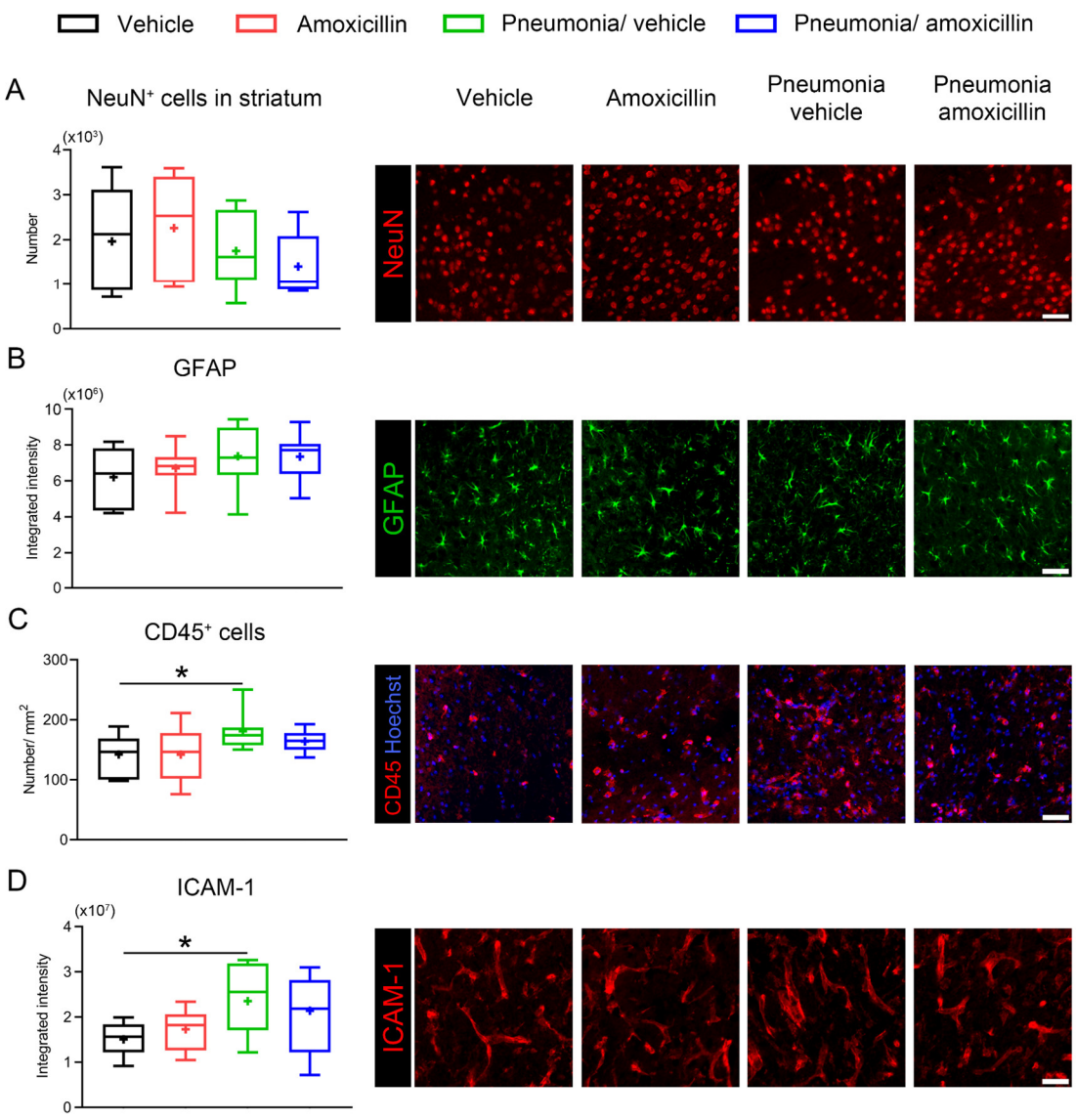

Figure 4. The impact of post-stroke pneumonia on neuron survival, astrocyte reactivity, leukocyte infiltration, and ICAM-1 expression.

(**A**) Neuronal survival, (**B**) astrocyte immunoreactivity, (**C**) peripheral leukocyte infiltration, and (**D**) ICAM-1 expression were evaluated at 2 dpp in mice exposed to 30 minutes intraluminal MCAO. The representative immunofluorescent staining images of NeuN, GFAP, CD45, and ICAM-1 are shown. Scale bars are 50 μm. *$p<0.05$ (n=7 animals/group).

3.3. Post-stroke pneumonia increases the formation of microthrombi

We also evaluated the formation of microthrombi within the ischemic hemisphere by immunofluorescent staining of GPIbα and collagen IV. When GPIbα positive aggregates were identified in collagen IV positive vessels, we considered them as microthrombi (**Figure 5A**). We analyzed the number and density of vessels with clots within the entire ipsilateral hemisphere, the cortex, and the striatum, respectively. The results show that post-stroke pneumonia significantly increased the formation of microthrombi in the ischemic hemisphere, cortex, and striatum (**Figure 5B-G**). According to some studies reported (Pham et al., 2010, Zhang et al., 2022)，the increase in thrombosis may be a reason of the exacerbation of neurological deficits, brain edema, and IgG extravasation. The treatment of pneumonia with amoxicillin significantly reduced the density of microthrombi in the ischemic hemisphere, cortex, and striatum, and also simultaneously reduced the number of microthrombi in the striatum (**Figure 5B, D, F, G**).

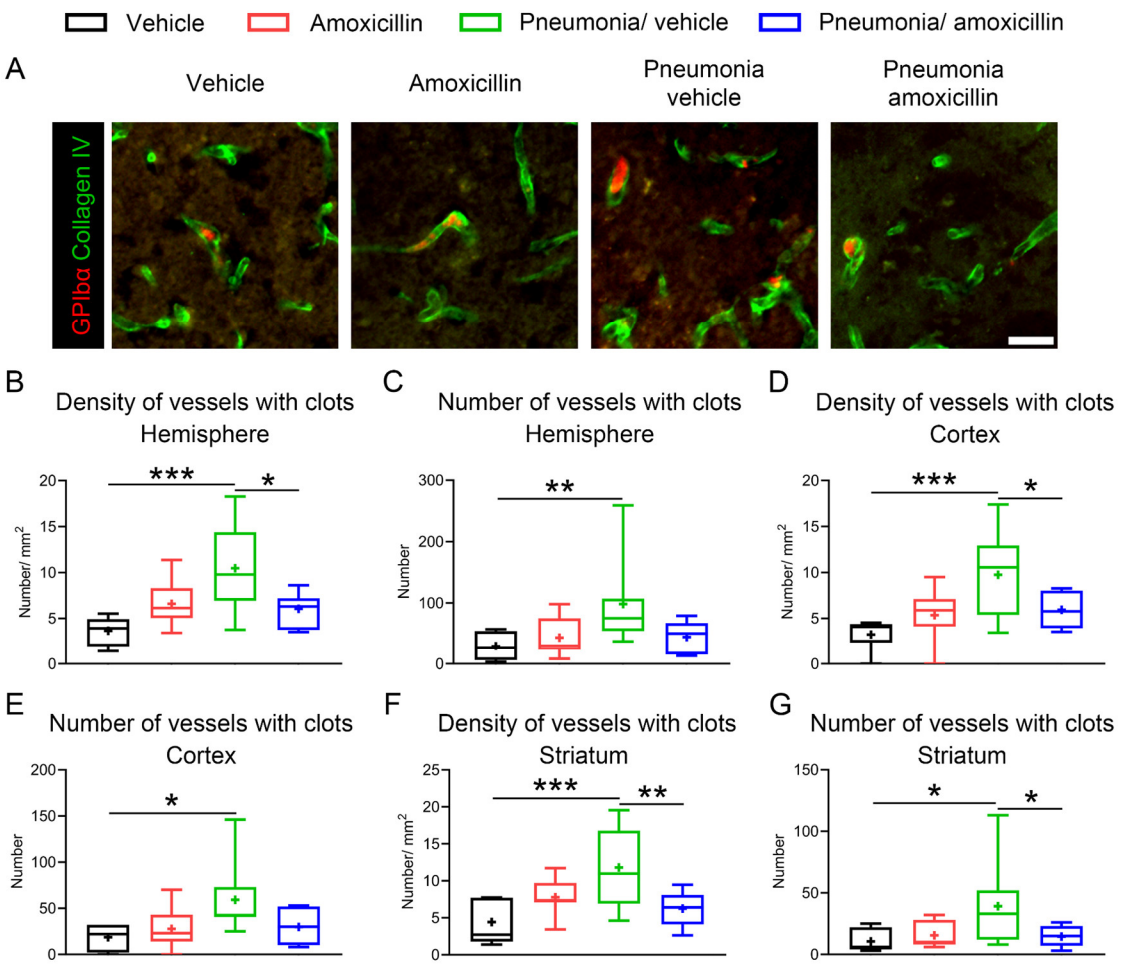

Figure 5. Post-stroke pneumonia increases microvascular thrombosis.

(**A**) Representative immunofluorescent staining of microthrombi, (**B-G**) density and number of vessels with clots in the ischemic hemisphere, cortex, and striatum at 2 dpp in mice exposed to 30 minutes intraluminal MCAO. Scale bar in (**A**) is 30 µm. *p<0.05, **p<0.01, ***p<0.001 (n=7 animals/group).

3.4. Post-stroke pneumonia decreases the number of microglia, and promotes the activation of microglia

As resident immune cell in the brain, impact of post-stroke pneumonia on microglia was also assessed. We evaluated the number and activation of microglia within the border of infarct, the core of infarct, and the entire infarct by combining border and core. The

representative images of microglia in the border and the core of the infarct are shown in **Figure 6A**. The results showed that post-stroke pneumonia did not significantly affect the density of microglia in the entire infarct or the border of infarct, but it significantly reduced the number of microglia in the infarct core. Treatment with amoxicillin did not show significant effects, but, compared to the pneumonia control group, significantly increased the number of microglia in the infarct core (**Figure 6B**). Following segmentation and skeletonization (**Figure 6C**), the activation of microglia was also statistically analyzed. For mice with stroke only, although amoxicillin significantly increased the territory volume and cell volume of microglia in the border of the infarct, it did not significantly affect the ramification index (**Figure 6D**). Pneumonia significantly reduced the ramification index in the border of infarct, thus promoting microglial activation, but additional treatment with amoxicillin restored the ramification index (**Figure 6D**). Similarly, in the core of the infarct, pneumonia significantly increased the cell volume of microglia, indicating their activation, whereas amoxicillin treatment attenuated cell volume (**Figure 6E**).

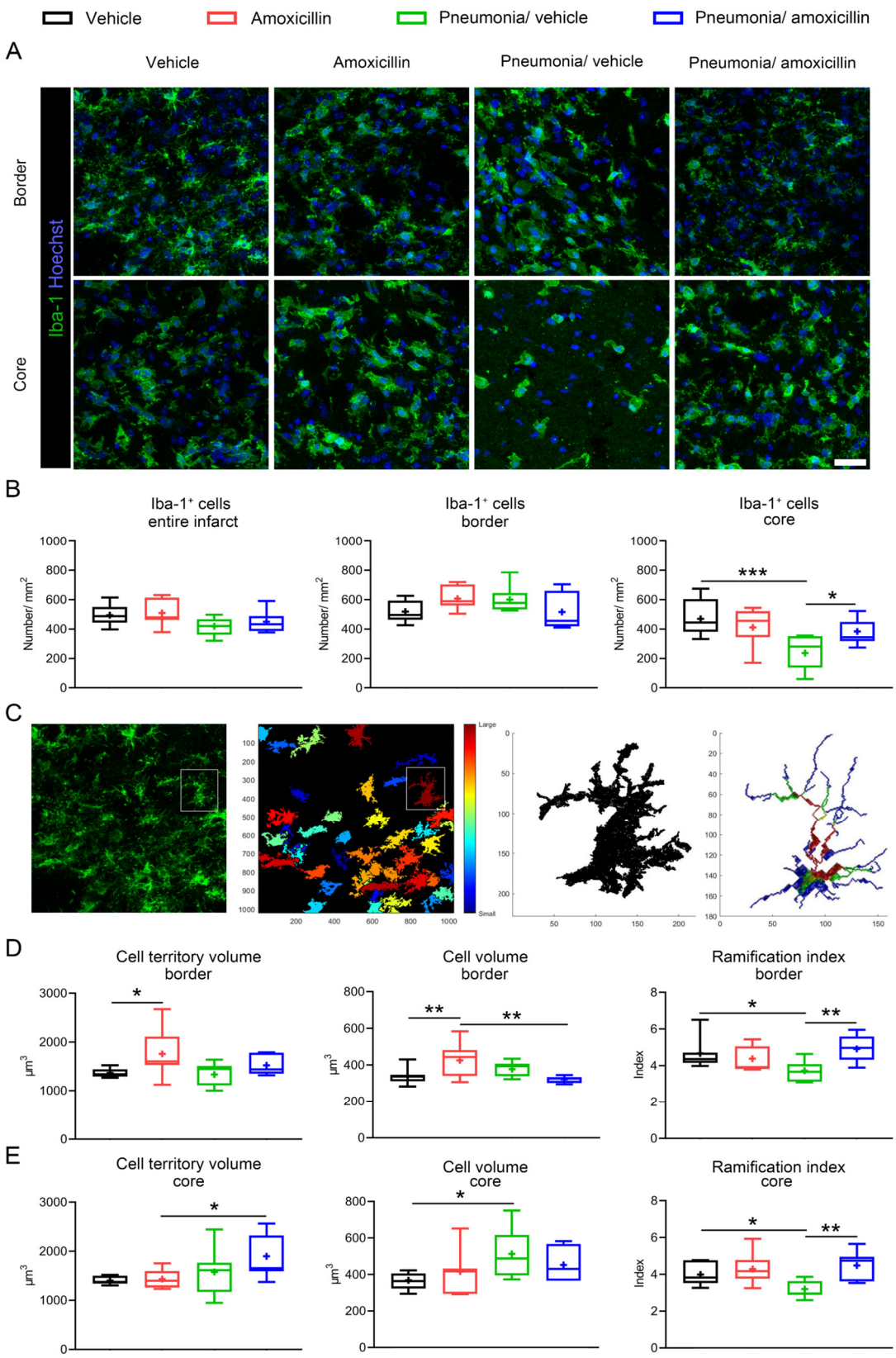

Figure 6 (for legend see subsequent page).

Figure 6 (for figure see previous page). Post-stroke pneumonia reduces the number of microglia in the core of infarct, and promotes activation of microglia in both the border and core of the infarct, which are reversed by amoxicillin treatment.

(**A**) Representative immunofluorescent staining of microglia in the infarct border and infarct core, (**B**) density of microglia in the entire infarct, in the infarct border, and in the infarct core, (**C**) representative images of segmentation and skeletonization for morphology, and (**D-E**) cell territory volume, cell volume and ramification index in the infarct border and in the infarct core at 2 dpp in mice exposed to 30 minutes intraluminal MCAO. Scale bar in (**A**) is 30 μm. *p<0.05, **p<0.01, ***p<0.001 (n=7 animals/group).

3.5. Post-stroke pneumonia increases the number of neutrophils in the blood, which is mitigated by amoxicillin treatment

At 2 dpp, flow cytometry analysis of leukocytes in peripheral blood showed that pneumonia occurring after stroke significantly increased the number of neutrophils (both activated and non-activated) and activated $CD8^+$ T cells in the blood, while simultaneously significantly reducing the number of activated $CD4^+$ T cells (**Figure 7**). In mice that experienced stroke only, the application of amoxicillin did not show any significant effects (**Figure 7**). However, compared to the control group with stroke and pneumonia, treatment of pneumonia with amoxicillin significantly reduced the number of neutrophils (both activated and non-activated), $CD4^+$ T cells, and $CD8^+$ T cells (**Figure 7**). Previous studies have shown that neutrophils are associated with thrombosis (Iba and Levy, 2018, von Bruhl et al., 2012). We hypothesized that the increase in brain microthrombosis may have been elicited by the increase and activation of microvascular blood neutrophils.

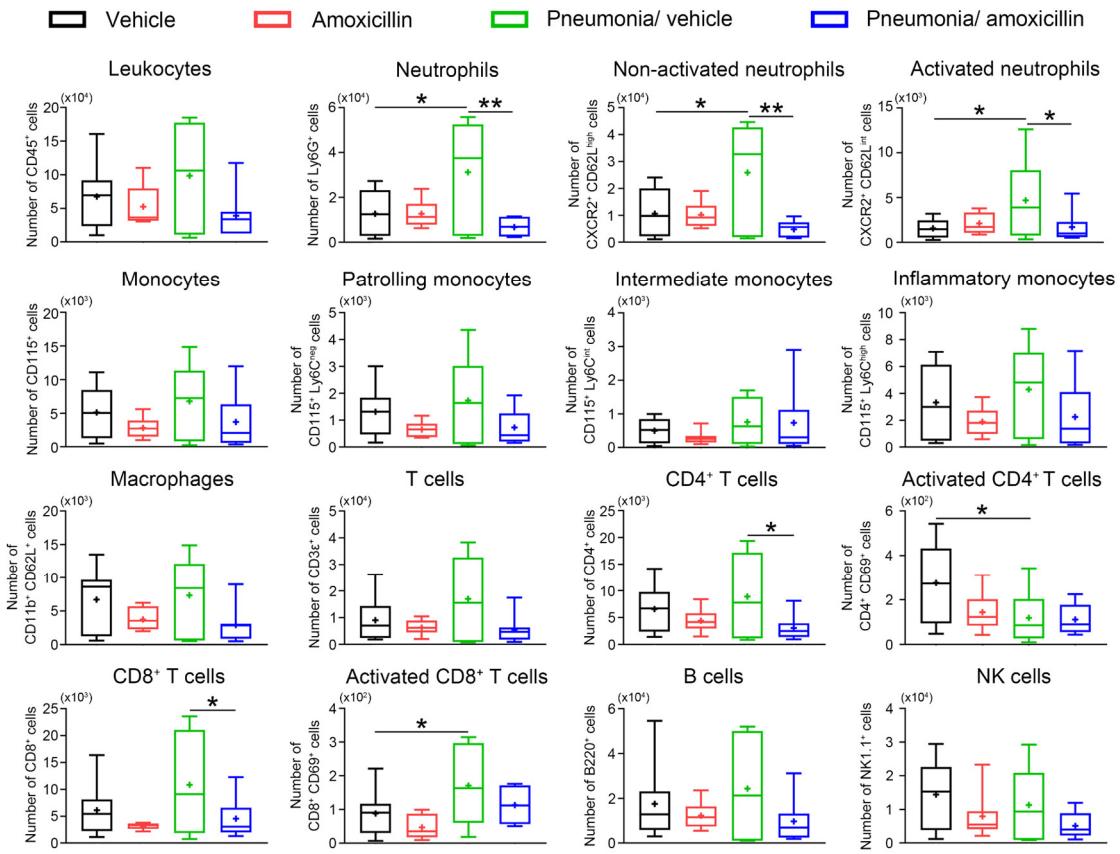

Figure 7. Flow cytometry results of leukocytes in blood samples at 2 dpp.

Leukocytes, including total $CD45^+$ leukocytes, $Ly6G^+$ neutrophils, $Ly6G^+$ $CXCR2^+$ $CD62L^{high}$ non-activated neutrophils, $Ly6G^+$ $CXCR2^+$ $CD62L^{int}$ activated neutrophils, $CD115^+$ monocytes, $CD115^+$ $Ly6C^{neg}$ patrolling monocytes, $CD115^+$ $Ly6C^{int}$ intermediate monocytes, $CD115^+$ $Ly6C^{high}$ inflammatory monocytes, $CD115^-$ $CD11b^+$ $CD62L^+$ macrophages, $CD3\varepsilon^+$ T cells, $CD4^+$ T cells, $CD4^+$ $CD69^+$ activated T cells, $CD8^+$ T cells, $CD8^+$ $CD69^+$ activated T cells, $B220^+$ B cells, and $NK1.1^+$ NK cells, in peripheral blood samples that from mice sacrificed at 2 dpp were analyzed by flow cytometry. *$p<0.05$, **$p<0.01$ (n=8 for vehicle group, 8 for amoxicillin group, 6 for pneumonia/ vehicle group, 8 for pneumonia/ amoxicillin group).

3.6. Post-stroke pneumonia increases the number of infiltrating leukocytes in brain, whereas amoxicillin treatment did not show any significant effects

As invaded leukocytes in brain were reported to contribute to ischemic brain injury after MCAO (Neumann et al., 2015), brain infiltrating leukocytes were also analyzed by flow cytometry at 2 dpp. The results showed that post-stroke pneumonia significantly increased the number of total leukocytes, neutrophils, non-activated neutrophils, monocytes, patrolling monocytes, intermediate monocytes, B cells, and NK cells in the brain (**Figure 8**). In mice with stroke only as well as mice with stroke and pneumonia, amoxicillin application did not show any significant effects on the number of leukocytes that infiltrating the brain (**Figure 8**).

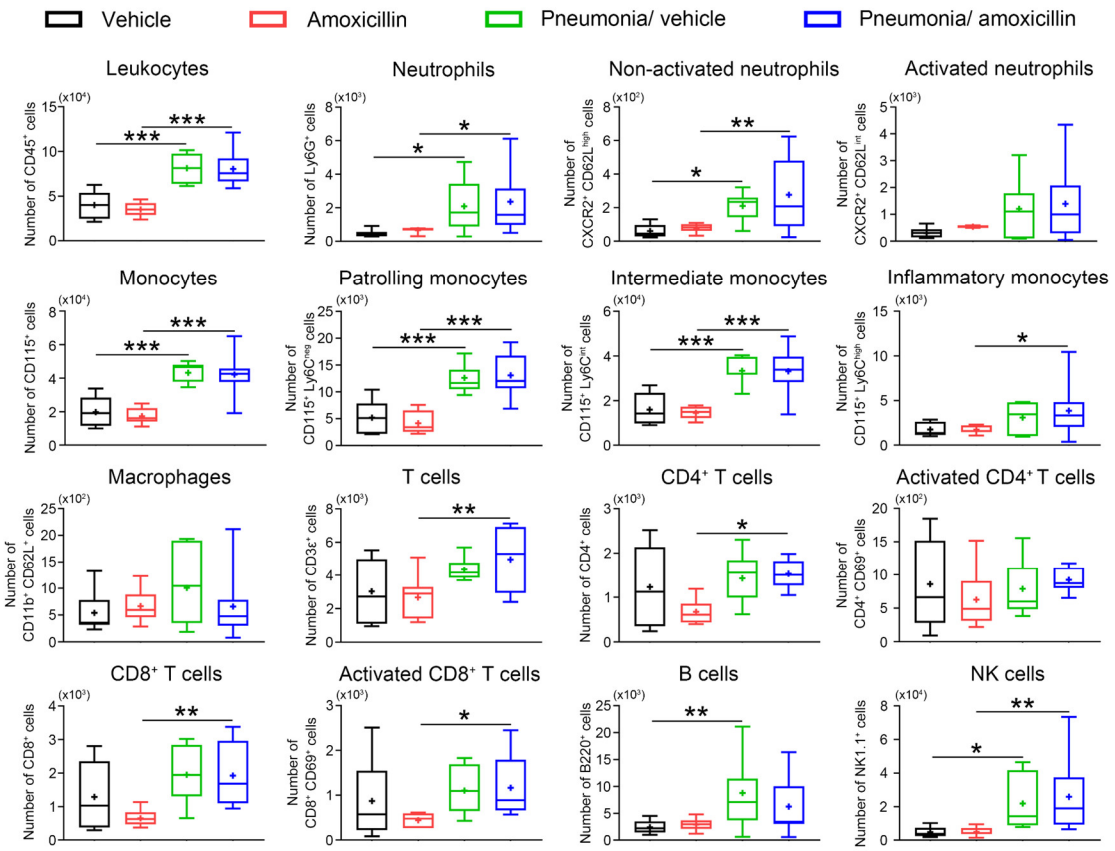

Figure 8. Flow cytometry results of brain infiltrating leukocytes at 2 dpp.

Infiltrating leukocytes, including total $CD45^+$ leukocytes, $Ly6G^+$ neutrophils, $Ly6G^+$

$CXCR2^+$ $CD62L^{high}$ non-activated neutrophils, $Ly6G^+$ $CXCR2^+$ $CD62L^{int}$ activated neutrophils, $CD115^+$ monocytes, $CD115^+$ Ly6Cneg patrolling monocytes, $CD115^+$ $Ly6C^{int}$ intermediate monocytes, $CD115^+$ Ly6Chigh inflammatory monocytes, $CD115^-$ $CD11b^+$ $CD62L^+$ macrophages, $CD3\varepsilon^+$ T cells, $CD4^+$ T cells, $CD4^+$ $CD69^+$ activated T cells, $CD8^+$ T cells, $CD8^+$ $CD69^+$ activated T cells, $B220^+$ B cells, and $NK1.1^+$ NK cells, in the brain of mice sacrificed at 2 dpp analyzed by flow cytometry. *p<0.05, **p<0.01, ***p<0.001 (n=8 for vehicle group, 8 for amoxicillin group, 7 for pneumonia/ vehicle group, 8 for pneumonia/ amoxicillin group).

3.7. Post-stroke pneumonia significantly worsens neurological deficits in the subacute stroke phase, and also significantly impairs the performance of animals in the rotarod test until the chronic phase

We have already reported the effects of post-stroke pneumonia on stroke during the acute stroke phase. Next, we aimed to explore whether it had any impact on the recovery from stroke in the subacute and chronic phase. We used the Clark score to evaluate the neurological deficits, and employed the tight rope test and rotarod test to assess the motor-coordination of animals up to 56 dpp. In the Clark score, pneumonia significantly worsened the performance of animals in the subacute phase. Amoxicillin treatment did not show significant effects in the subacute phase, but provided improvement at 42 dpp and 56 dpp (**Figure 9A**). For the tight rope test, both pneumonia and amoxicillin treatment did not show any significant effect across all phases (**Figure 9B**). In the rotarod test, however, pneumonia significantly worsened the performance of animals at all time points, while amoxicillin treatment did not show any significant improvement (**Figure 9C**).

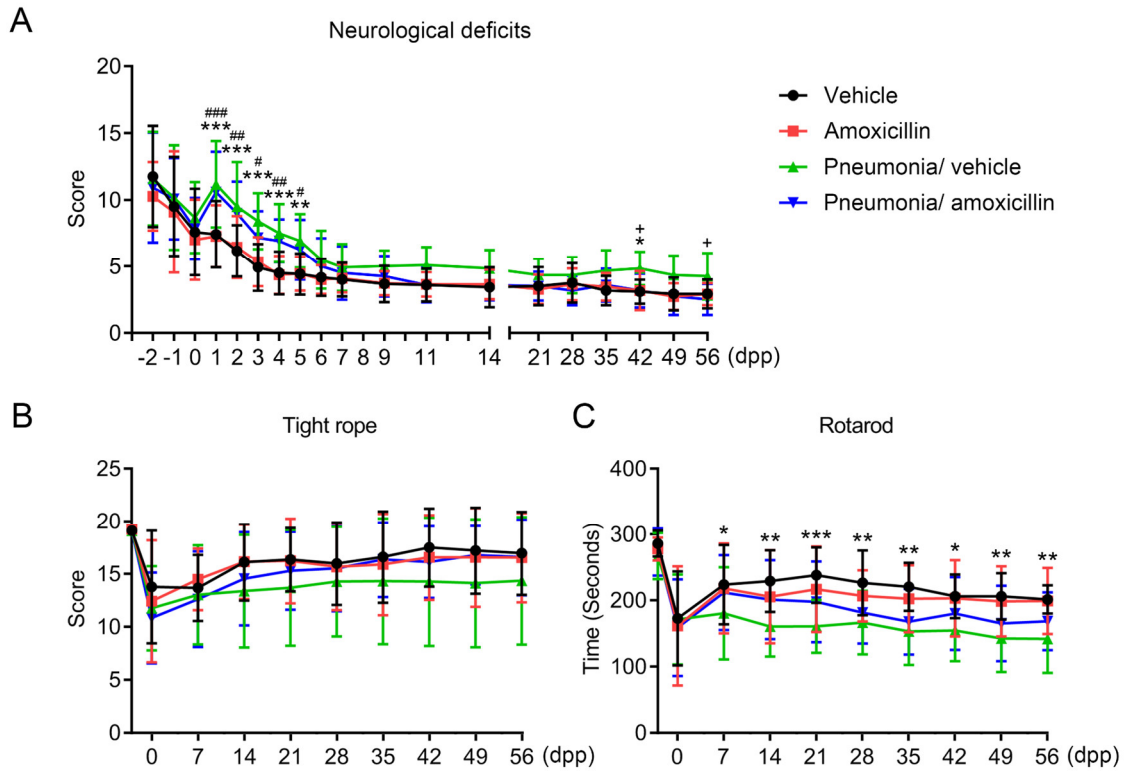

Figure 9. Post-stroke pneumonia worsens neurological deficits mainly in the subacute stroke phase and impairs motor coordination in all phases.

(**A**) Neurological deficits evaluated by the Clark score, motor coordination assessed by the (**B**) tight rope test, and (**C**) rotarod test were assessed up to 56 dpp. * indicates the comparison between pneumonia/ vehicle group and vehicle group, # indicates the comparison between pneumonia/ amoxicillin group and amoxicillin group, + indicates the comparison between pneumonia/ amoxicillin group and pneumonia/ vehicle group. *p<0.05, **p<0.01, ***p<0.001, #p<0.05, ##p<0.01, ###p<0.001, +p<0.05. (n=12 for vehicle group, 12 for amoxicillin group, 11 for pneumonia/ vehicle group, 12 for pneumonia/ amoxicillin group)

3.8. Post-stroke pneumonia significantly increases brain atrophy and striatal atrophy in the chronic phase, and increases the reactivity of astrocytes

At 7 dpp, 14 dpp, and 56 dpp, brain atrophy and striatal atrophy were assessed using

cresyl violet staining, while neuronal survival and astrocyte activation were evaluated by immunofluorescence staining. The results showed that post-stroke pneumonia aggravated brain atrophy (**Figure 10A**) and striatal atrophy (**Figure 10B**) at 7 dpp and 56 dpp. Post-stroke pneumonia did not affect the neuronal survival in the striatum (**Figure 10C**), but increased astrocyte reactivity (**Figure 10D**) at 7 dpp and 14 dpp. Amoxicillin treatment post pneumonia mitigated brain atrophy (**Figure 10A**) and striatal atrophy (**Figure 10B**) at 56 dpp, but showed no effects on neuronal survival in the striatum (**Figure 10C**) and astrocyte reactivity (**Figure 10D**).

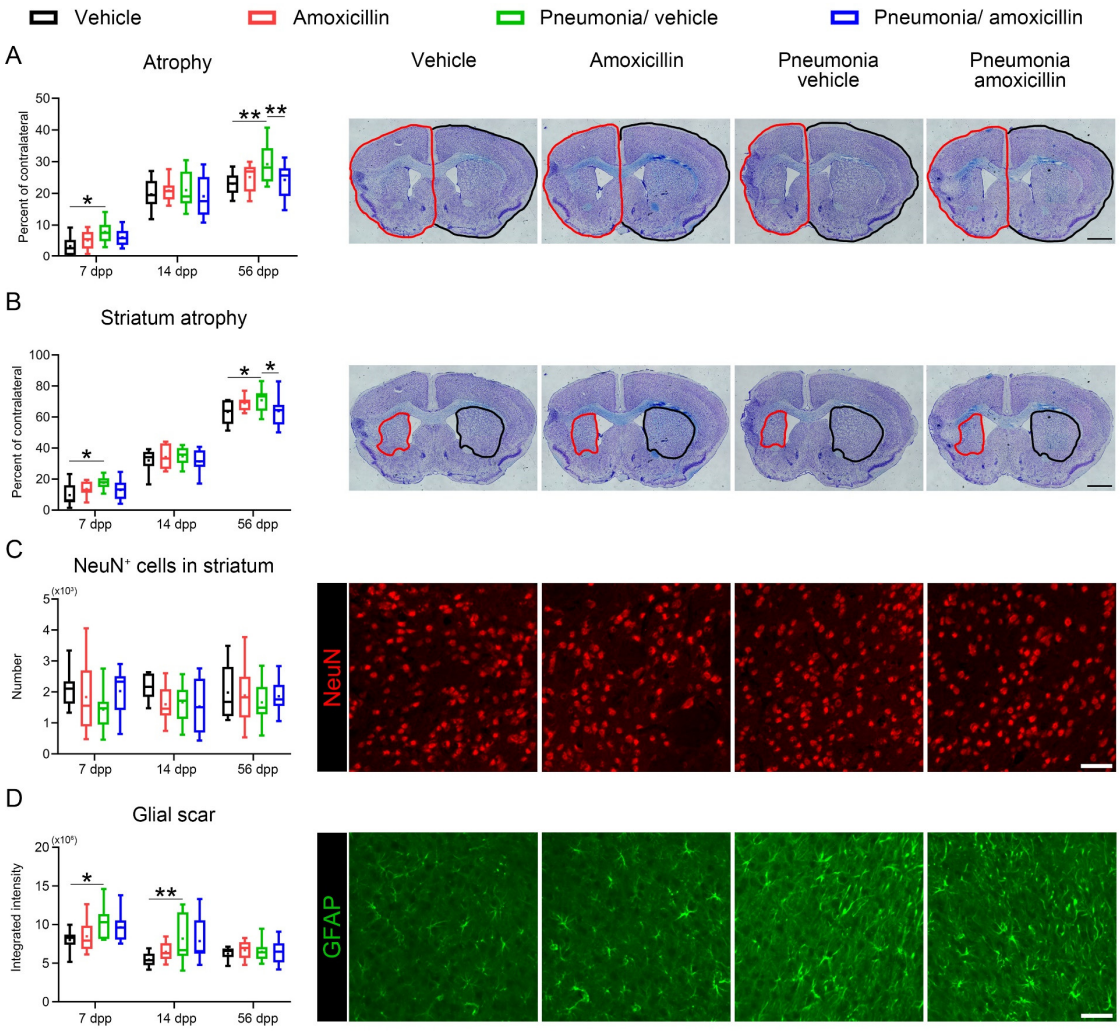

Figure 10 (for legend see subsequent page).

Figure 10 (for figure see previous page). Post-stroke pneumonia exacerbates brain and striatal atrophy, and increases astrocyte reactivity.

(**A**) Brain atrophy and (**B**) striatal atrophy were evaluated via cresyl violet staining, (**C**) neuronal survival and (**D**) astrocyte reactivity were evaluated by immunofluorescent staining in brain sections obtained from mice at 7 dpp, 14 dpp and 56 dpp. Representative images are shown. Scale bars in (**A**) and (**B**) are 1 mm, in (**C**) and (**D**) are 50 µm. *p<0.05, **p<0.01 (for 7 dpp, n=8 for vehicle group, 9 for amoxicillin group, 8 for pneumonia/ vehicle group, 9 for pneumonia/ amoxicillin group; for 14 dpp, n=8 for each group; for 56 dpp, n=12 for vehicle group, 12 for amoxicillin group, 11 for pneumonia/ vehicle group, 12 for pneumonia/ amoxicillin group).

3.9. Neutrophil depletion alleviates the detrimental effects of post-stroke pneumonia

Based on previously published articles (Jickling et al., 2015, Yan et al., 2023) and the results of the former experiments in this study, we hypothesized that the deleterious effects of pneumonia were associated with the increase in circulating neutrophils and the rise in microthrombus formation. Consequently, we depleted neutrophils prior to pneumonia. Initiating neutrophil depletion one day before pneumonia, which is two days post-stroke, did not result in any significant changes at 2 dpp in animals that were exposed to stroke (**Figure 11** and **Figure 12**). However, in mice with post-stroke pneumonia, neutrophil depletion, while not inducing significant alterations in neurological deficits (**Figure 11A**), neuronal survival (**Figure 12A**), and ICAM-1 expression (**Figure 12B**), significantly mitigated cerebral infarct volume (**Figure 11B**), brain edema (**Figure 11C**), IgG extravasation (**Figure 11D**), and the formation of microthrombi within the infarct (**Figure 12C, D**) compared to the control group. These results indicate that neutrophils are important mediating of the unfavorable effects of post-stroke pneumonia.

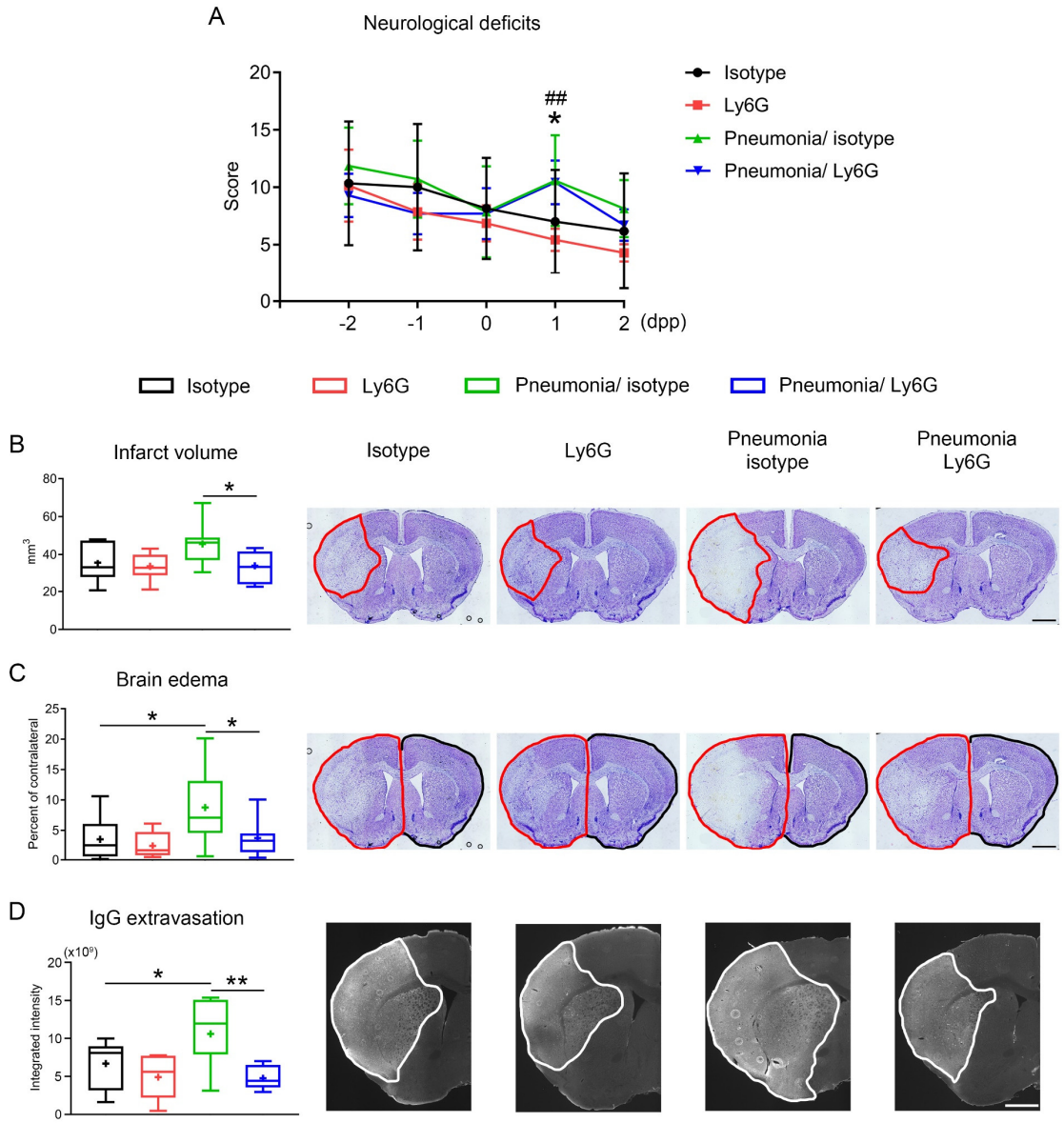

Figure 11. Neutrophil depletion mitigates infarct volume, brain edema and IgG extravasation in mice with stroke-associated pneumonia.

(**A**) Neurological deficits were assessed by Clark score, (**B**) infarct volume and (**C**) brain edema were evaluated by cresyl violet staining, (**D**) IgG extravasation was evaluated by immunofluorescent staining in brain sections obtained from mice at 2 dpp. Representative images are show. Scale bars in (**B**), (**C**) and (**D**) are 1 mm. * in (**A**) indicates the comparison between pneumonia/ isotype and isotype groups, # indicates

the comparison between pneumonia/ Ly6G and Ly6G groups. *p<0.05, **p<0.01, ##p<0.01 (n=6 for isotype group, 7 for Ly6G group, 7 for pneumonia/ isotype group, 7 for pneumonia/ Ly6G group).

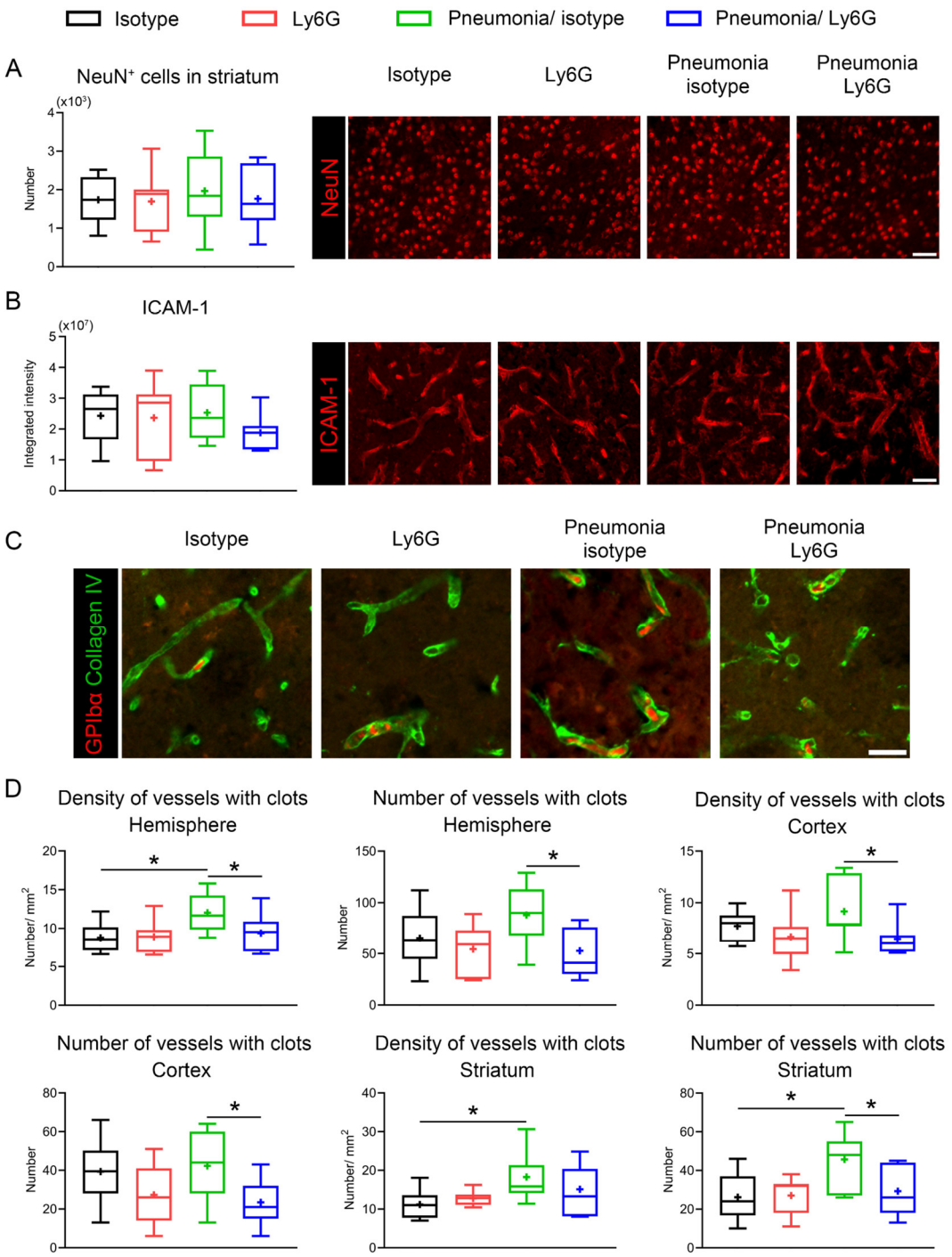

Figure 12 (for legend see subsequent page).

Figure 12 (for figure see previous page). Neutrophil depletion alleviates post-ischemic microthrombosis.

Immunofluorescent staining was employed at 2 dpp to analyze (**A**) neuronal survival, (**B**) microvascular ICAM-1 expression and (**C, D**) microthrombus formation in the ischemic hemisphere, cortex, and striatum. Representative images are shown. Scale bars in (**A**) and (**B**) are 50 μm, in (**C**) is 30 μm. *$p<0.05$ (n=6 for isotype group, 7 for Ly6G group, 7 for pneumonia/ isotype group, 7 for pneumonia/ Ly6G group).

3.10. DNase I has no significant effect on stroke outcome, but increases brain hemorrhage formation

NETs, derived from neutrophils, have been demonstrated to promote thrombosis (von Bruhl et al., 2012), and some studies in recent years have suggested that NETs impair ischemic stroke outcome (Denorme et al., 2022, Kang et al., 2020). Therefore, following the observation of an association between neutrophils and the unfavorable effects of post-stroke pneumonia, we further investigated the role of NETs in this process. Our findings revealed that administration of DNase I 30 minutes prior to pneumonia did not significantly influence neurological deficits (**Figure 13A**), infarct volume (**Figure 13B**), brain edema (**Figure 13C**), IgG extravasation (**Figure 13D**), neuronal survival (**Figure 14A**), ICAM-1 expression (**Figure 14B**), and microthrombosis (**Figure 14C, D**) at 2 dpp. Importantly, the injection of DNase I significantly increased brain hemorrhage formation at 2 dpp, an effect observed in mice with both pneumonia and stroke, as well as in mice with stroke only (**Figure 14E**).

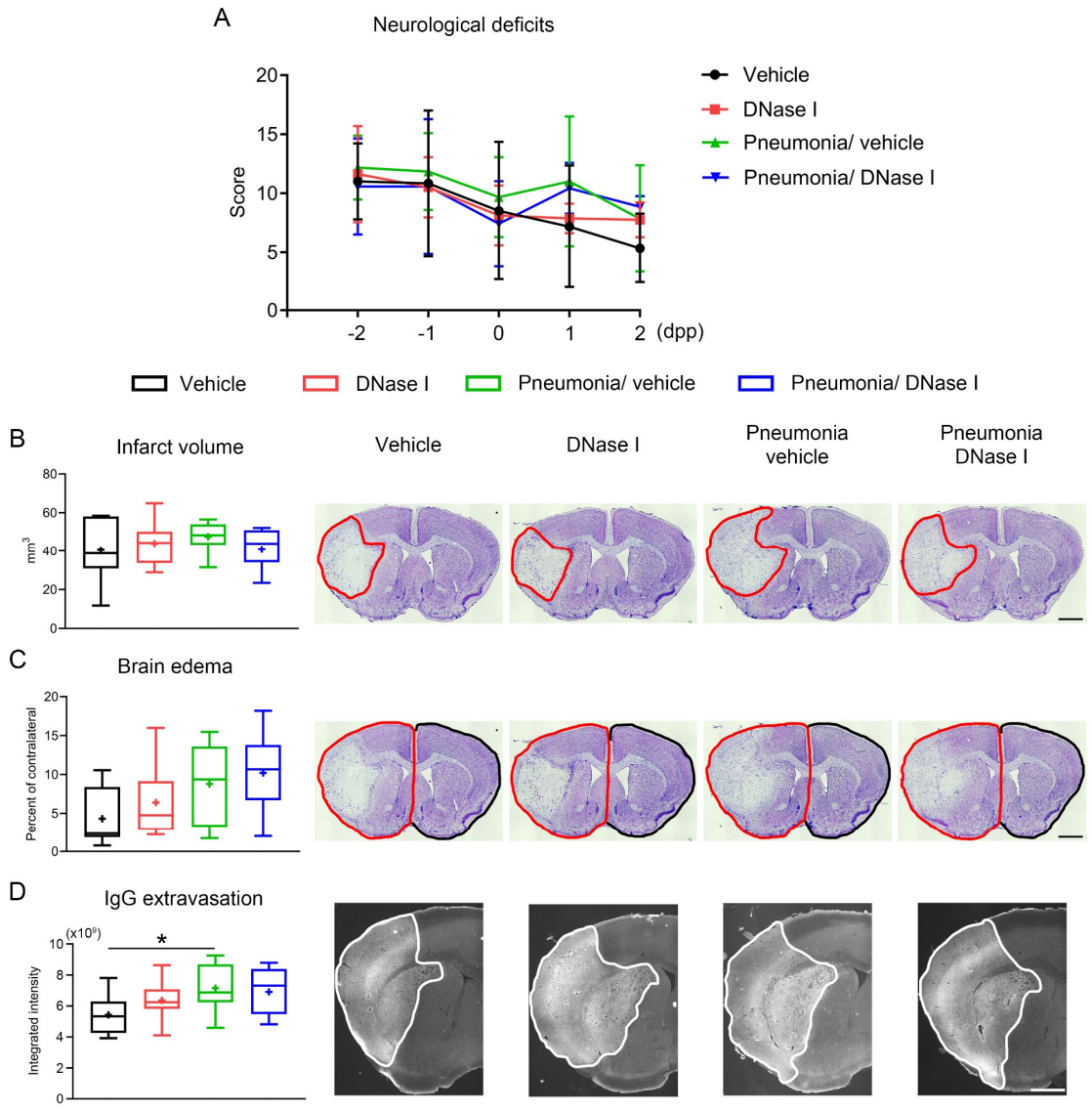

Figure 13. DNase I injection does not show significant effects on neurological deficits, brain volume, brain edema, and IgG extravasation in mice with post-stroke pneumonia.

(**A**) Neurological deficits, (**B**) infarct volume and (**C**) brain edema that evaluated by cresyl violet staining, (**D**) IgG extravasation that evaluated by immunofluorescent staining on brain tissues obtained from mice at 2 dpp. Representative images of the staining are show. Scale bars in (**B**), (**C**) and (**D**) are 1 mm. *$p<0.05$ (n=6 for vehicle group, 8 for DNase I group, 6 for pneumonia/ vehicle group, 7 for pneumonia/ DNase I group).

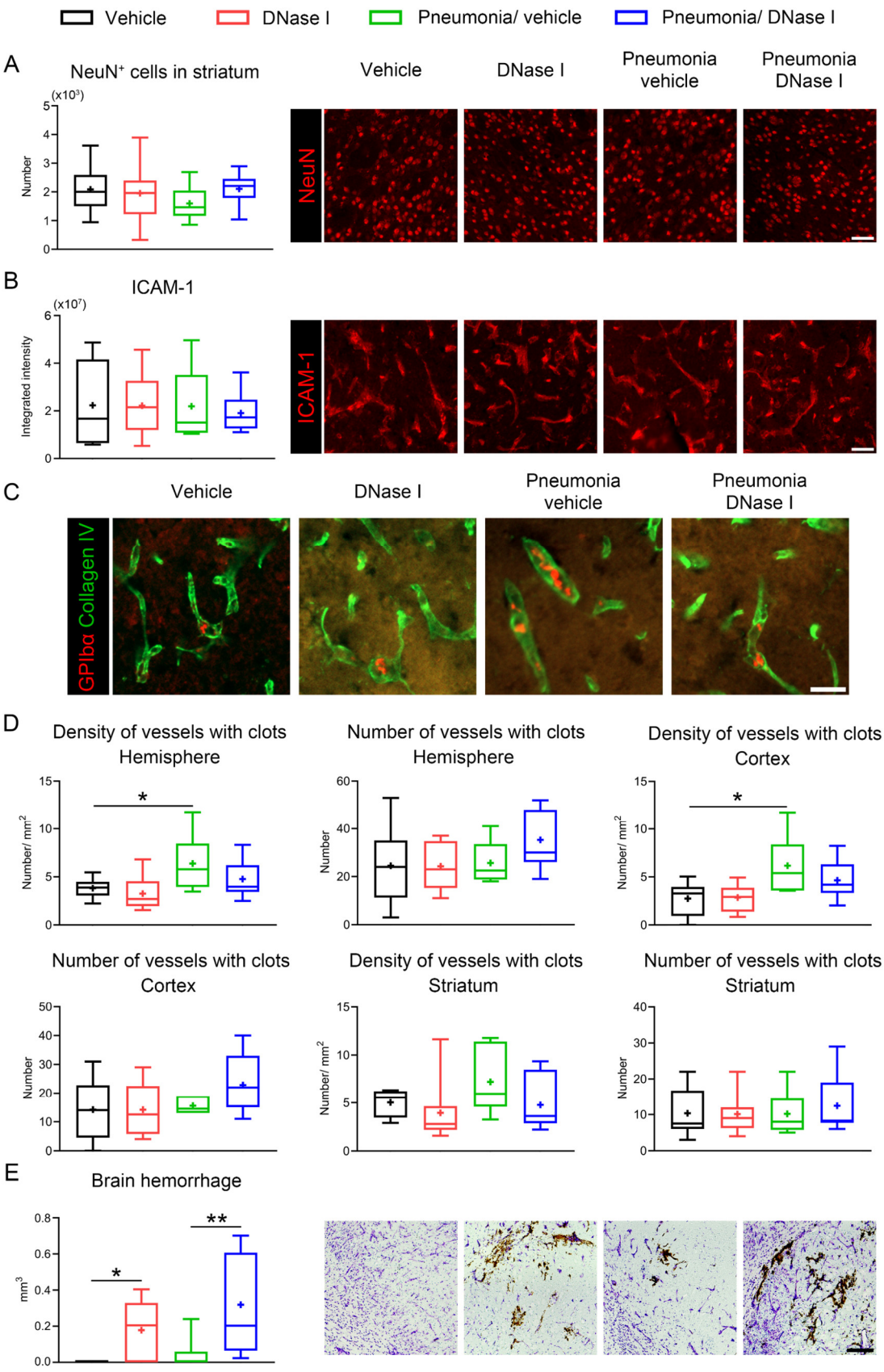

Figure 14 (for legend see subsequent page)

Figure 14 (for figure see previous page). DNase I injection does not significantly reduce brain microthrombosis, but significantly increases brain hemorrhage formation.

(**A**) Neuronal survival, (**B**) ICAM-1 expression and (**C, D**) microthrombi within the ischemic hemisphere, cortex, and striatum were evaluated by immunofluorescent staining, (**E**) hemorrhage formation was analyzed by DAB staining in brain sections obtained from mice at 2 dpp. Representative images are show. Scale bars in (**A**) and (**B**) are 50 μm, in (**C**) is 30 μm, in (**E**) is 200 μm. *p<0.05, **p<0.01 (n=6 for vehicle group, 8 for DNase I group, 6 for pneumonia/ vehicle group, 7 for pneumonia/ DNase I group).

3.11. LDC7559 injection reduces the levels of NETs in blood, and reduces brain edema and IgG extravasation

Following the unsuccessful attempt with DNase I treatment, we turned our attention to the gasdermin D inhibitor LDC7559, a compound reported in recent years to inhibit NET formation (Amara et al., 2021, Sollberger et al., 2018). Our results again showed that post-stroke pneumonia significantly elevated the levels of NETs in the blood (**Figure 15A**). LDC7559 injection 30 minutes before pneumonia significantly reduced NET levels in the blood (**Figure 15A**). Although LDC7559 treatment in mice with stroke only or in mice with stroke and post-stroke pneumonia did not significantly improve neurological deficits (**Figure 15B**), infarct volume (**Figure 15C**), brain edema (**Figure 15D**), IgG extravasation (**Figure 15E**), neuronal survival (**Figure 16A**), and ICAM-1 expression (**Figure 16B**) at the time points examined, LDC7559 treatment significantly reduced the density of vessels with microthrombi in the striatum, but no significant differences were observed in other measures (**Figure 16C, D**).

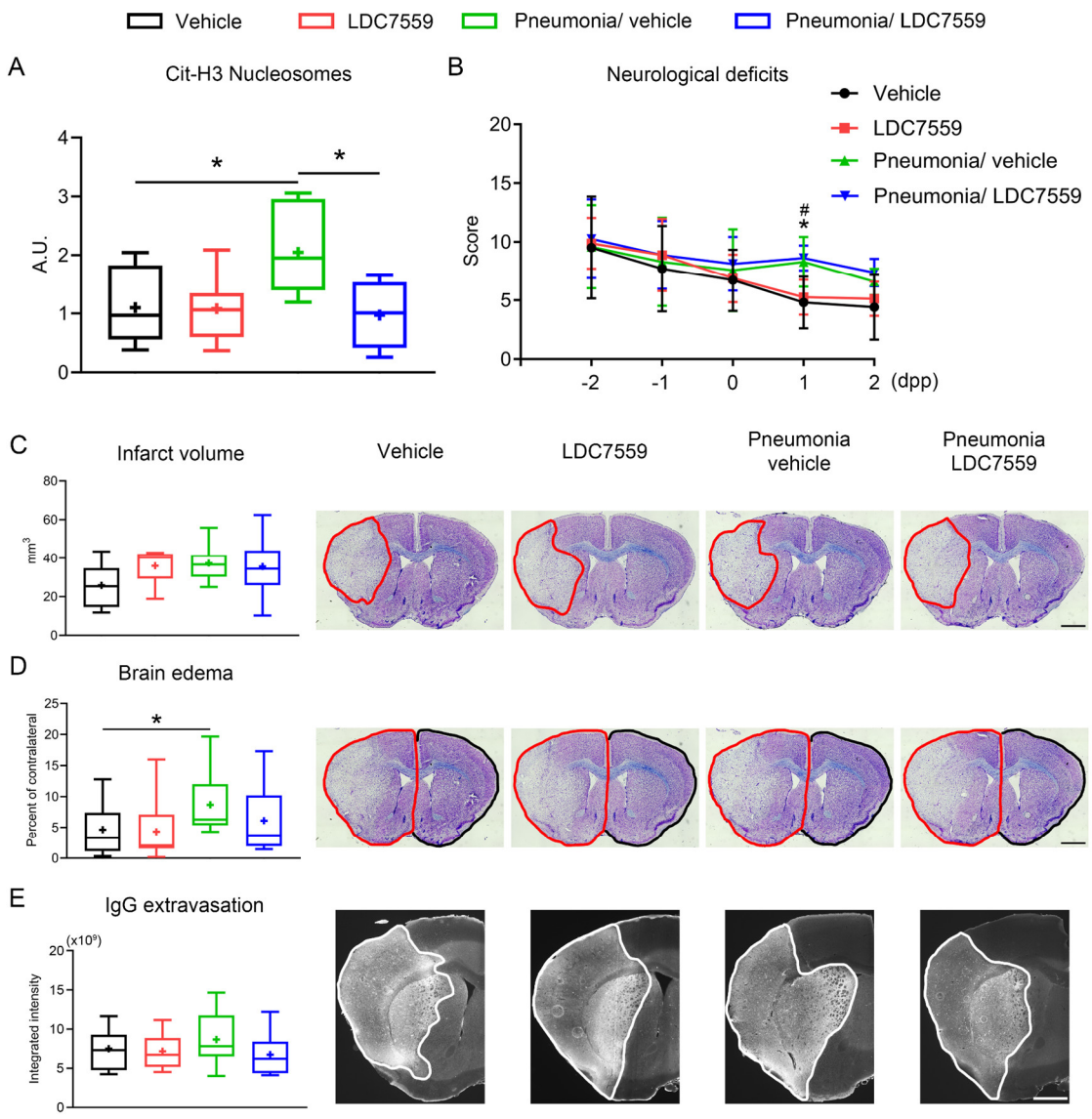

Figure 15. LDC7559 treatment decreases the NET levels in the blood, and attenuates brain edema and IgG extravasation.

(**A**) NET levels in the blood were assessed by ELISA, (**B**) neurological deficits were evaluated by Clark score, (**C**) infarct volume and (**D**) brain edema were evaluated by cresyl violet staining, (**E**) IgG extravasation was evaluated by immunofluorescent staining in brain sections obtained from mice at 2 dpp. Representative images are shown. * in **(B)** indicates the comparison between pneumonia/ vehicle and vehicle groups, # indicates the comparison between pneumonia/ LDC7559 and LDC7559 groups. Scale bars in (**C**), (**D**) and (**E**) are 1 mm. *p<0.05 (n=10 for vehicle group, 8 for LDC7559

group, 7 for pneumonia/ vehicle group, 8 for pneumonia/ LDC7559 group).

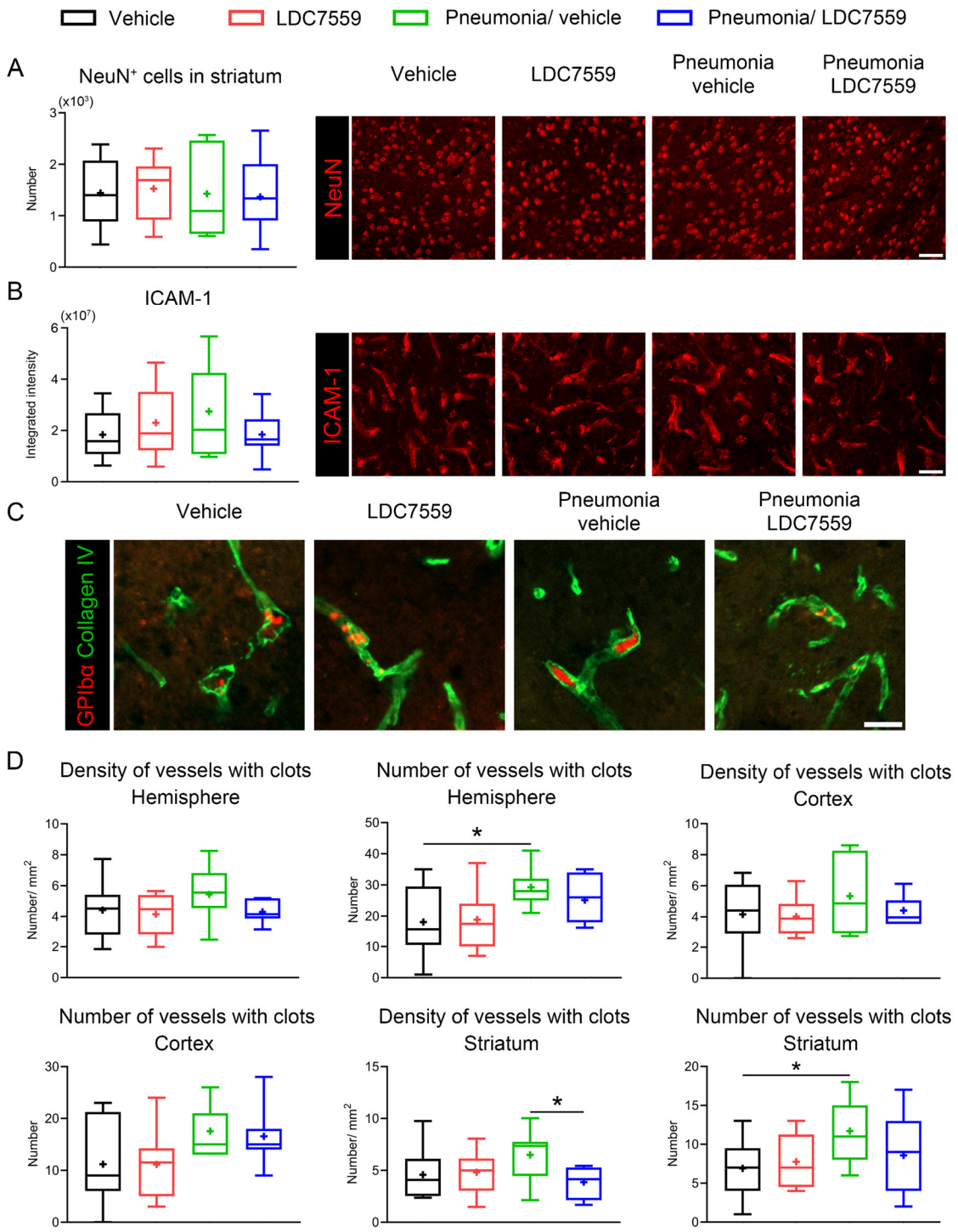

Figure 16 (for legend see subsequent page).

Figure 16 (for figure see previous page). LDC7559 injection does not influence neuronal survival and ICAM-1 expression, but significantly decreases the density of vessels with clots.

(**A**) Neuronal survival, (**B**) ICAM-1 expression and (**C, D**) microthrombi including the number and density of vessels with clots throughout the entire infarct, cortex, and striatum were evaluated by immunofluorescent staining in brain sections at 2 dpp. Representative images are shown. Scale bars in (**A**) and (**B**) are 50 μm, in (**C**) is 30 μm. *$p<0.05$ (n=10 for vehicle group, 8 for LDC7559 group, 7 for pneumonia/ vehicle group, 8 for pneumonia/ LDC7559 group).

4. DISCUSSION

In this study, we explored the impact of pneumonia that was experimentally induced after ischemic stroke on ischemic injury and stroke recovery. The results indicated that during the acute phase, although pneumonia induced post-stroke did not significantly alter the infarct volume, it markedly exacerbated the neurological deficits following stroke, promoted cerebral edema and IgG extravasation, increased the infiltration of peripheral leukocytes in the brain parenchyma, and elevated the expression of ICAM-1 on microvessels. These results indicated that pneumonia exacerbates brain injury by increasing blood-brain barrier damage and inflammatory responses in the brain. The improvements brought about by the antibiotic amoxicillin were not significant, showing only a slight trend towards alleviation. Our findings also demonstrated that pneumonia following ischemic stroke significantly increased brain atrophy and neurological deficits in the subacute and chronic phase, as well as impaired overall performance in the rotarod test. Amoxicillin treatment significantly reduced cerebral atrophy and improved neurological deficits evaluation, but the improvement of neurological deficits and behavioral performance was not significant.

Our study revealed that microglia, the resident immune cells of the central nervous system, exhibited a significant decrease in number within the core of the brain infarct in response to post-stroke pneumonia. Concurrently, microglial activation significantly increased in both the infarct core and border by post-stroke pneumonia. The treatment of pneumonia with amoxicillin effectively mitigated these changes. Previous studies have indicated that following ischemic stroke, microglia within the core region decreased in response to ischemia and hypoxia (Matsumoto et al., 2007), but approximately 24-48 hours after reperfusion, the number of microglia in this region began to increase (Ito et al., 2001, Zhang et al., 1997). However, in our experiments, the occurrence of pneumonia notably reduced the number of microglia within the infarct core at 2 dpp (5 days post-stroke) and elevated their activation level. Associated with a rise in microvascular ICAM-1 expression levels and increased infiltration of peripheral

leukocytes, these findings suggest that post-stroke pneumonia exacerbates local brain inflammatory responses and brain injury, thus impeding stroke recovery. The treatment with amoxicillin did not reverse the consequences of pneumonia.

We also observed that pneumonia following ischemic stroke significantly increased the formation of microthrombi in previously ischemic brain vessels, and that treatment of pneumonia with amoxicillin significantly reduced these microthrombi. In clinical patients, infarct volume may still increase even after successful recanalization through thrombolysis or thrombectomy, a process attributed to secondary ischemia-reperfusion damage (Stoll and Nieswandt, 2019). Although the specific mechanisms underlying this secondary infarct growth remain unclear, thrombo-inflammation may play a critical role in this process (Schuhmann et al., 2017, Stoll and Nieswandt, 2019). We here provide experimental proofs that substantiate this hypothesis that thrombus formation contributes to secondary brain injury.

Subsequently, we conducted flow cytometry analyses on brain tissue and blood samples of mice at 2 dpp. Our results indicated that post-stroke pneumonia affected the numbers of various leukocyte subtypes in the blood, with a particularly notable increase in the number and activation of neutrophils. Treatment with amoxicillin was able to significantly reduce the pneumonia-induced increase in neutrophil numbers. However, in brain tissues, amoxicillin treatment did not mitigate the increase of infiltrating leukocytes evoked by pneumonia. Notably, our analysis of blood samples using flow cytometry revealed a consistency between the results of neutrophils and the results of microthrombi. In line with findings from various studies that neutrophils are closely associated with thrombus formation (Darbousset et al., 2012, Darbousset et al., 2014, Pircher et al., 2019), we hypothesized that pneumonia might exacerbate brain injury by increasing the number and activation of circulating neutrophils, thereby augmenting the formation of microthrombi in brain infarcts. Existing research suggests that the mechanism by which pneumonia aggravates post-stroke brain injury may be related to an increase in microthrombus formation (Denes et al., 2014). Our findings further

suggest that this increase in microthrombi may be closely related to the rise in circulating neutrophils caused by pneumonia. To test this hypothesis, we proceeded with experiments involving the depletion of neutrophils.

One day before the induction of pneumonia, which was the second day after the ischemic stroke, we initiated the depletion of neutrophils in mice and subsequently euthanized them at 2 dpp for further experimental analyses. Our results demonstrated that in the only stroke group, neutrophil depletion did not yield any noticeable improvement. This finding is different to some previous studies indicating that neutrophil depletion could ameliorate brain damage post ischemic stroke (Neumann et al., 2015, Yan et al., 2023). The discrepancy could likely be attributed to the timing of our intervention. Previous research had initiated neutrophil depletion before the onset of ischemia (Neumann et al., 2015, Yan et al., 2023), whereas our depletion protocol was conducted 48 hours post-stroke. Considering that neutrophils are the first peripheral immune cells to infiltrate the brain tissue after a stroke, reaching a peak infiltration within 24 to 48 hours post-stroke (Jickling et al., 2015, Hermann and Gunzer, 2019), our timing for neutrophil depletion might have missed this critical window, leading to the ineffectiveness of the intervention. However, in mice that concurrently suffered from pneumonia, our intervention of neutrophil depletion significantly reduced the volume of infarct, decreased the permeability of the blood-brain barrier, and lowered the number of microthrombi. Despite this, our neutrophil depletion strategy failed to ameliorate neurological deficits. Pneumonia is a severe infectious condition, and neutrophil depletion might have interfered with the recovery process from pneumonia, subsequently affecting the overall condition of the mice and potentially covered any improvements in neurological function. This is the limitation of the neutrophil depletion strategy. As the most abundant type of leukocytes in the human blood, neutrophils play a crucial role in the defense against infections, which precludes the clinical translation of this neutrophil depletion strategy in humans.

Therefore, we shifted our focus towards NETs, which are closely associated with

neutrophils. NETs are web-like structures formed by DNA, histones, and other cellular contents released by activated neutrophils (Thakur et al., 2023, Zhao et al., 2023). They play a role in capturing and eliminating a wide range of pathogens (Papayannopoulos, 2018), but are also implicated in thrombosis formation (Fuchs et al., 2010). Studies have shown that NETs can affect post-stroke revascularization, detrimentally influencing recovery from ischemic stroke (Kang et al., 2020). Given that DNA is a critical component of NETs, some research has explored the use of DNase I post-stroke to degrade NETs. Animal experiments have indicated that DNase I treatment can improve outcomes in mice with cerebral infarction (Kang et al., 2020, Denorme et al., 2022), and studies by Laridan et al. have found that DNase I can enhance the in vitro dissolution of clots extracted from stroke patients mediated by tPA (Laridan et al., 2017). Thus, our initial approach was to employ DNase I intervention to observe its therapeutic effect on post-stroke pneumonia. Our results demonstrated that DNase I treatment not only failed to provide any improvement but also increased the incidence of brain hemorrhages. Notably, earlier studies have suggested that DNase I application could reduce brain damage post-infarction (Kang et al., 2020, Denorme et al., 2022) and, when used in conjunction with tPA, could lower the risk of hemorrhages induced by tPA (Wang et al., 2021). However, these experiments administered DNase I either before the stroke or shortly thereafter, whereas our treatment was initiated 3 days post-ischemia. This difference in timing of administration likely accounts for the different outcomes. It is conceivable that, similar to tPA, DNase I treatment has a strict therapeutic window. Administration beyond this window not only fails to bring benefits but may also increase the risk of adverse effects. Currently, there are three randomized controlled clinical trials performed in human stroke patients, which evaluate the effects of DNase I (NCT05203224, NCT05880524, and NCT04785006). These studies have to be aware of this potential deleterious action.

After the unsuccessful treatment attempts with DNase I, we shifted our attention towards LDC7559. LDC7559 is a small molecule compound reported in recent years to

inhibit the formation of NETs. Despite existing controversy over the precise mechanism through which it inhibits NET formation—a study suggested its action is mediated through the inhibition of gasdermin D (Sollberger et al., 2018), while another study attributes its effects primarily to the suppression of reactive oxygen species (ROS) (Stojkov et al., 2023)—the inhibitory impact of LDC7559 on NETs formation is well documented in the literature (Sollberger et al., 2018, Amara et al., 2021). 30 minutes prior to the induction of pneumonia, mice received LDC7559, which significantly reduced the levels of CitH3 in the blood compared to the pneumonia control group. However, the application of LDC7559 did not ameliorate neurological deficits, but reduced, although not significantly, cerebral edema and IgG extravasation. LDC7559 induced a significant reduction of the increased thrombus formation in mice with stroke-associated pneumonia. Overall, the application of LDC7559 mitigated the unfavorable effects associated with post-stroke pneumonia, indicating its possible therapeutic clinical potential. Additional studies are currently put forward to increase animal numbers and evaluate long-term consequences of LDC7559 delivery in the post-stroke pneumonia model. As a novel small molecule compound, the specific dosage, timing of application, and mechanisms of LDC7559 in the treatment of stroke and post-stroke pneumonia require further investigation.

This study also has several limitations. We so far did not conduct long-term experiments on the effects of neutrophil depletion, DNase I, and LDC7559 yet. Thus, their roles in facilitating long-term recovery in the mouse model of post-stroke pneumonia remain to be shown. Additionally, while neutrophil depletion significantly reduced thrombus formation and helped alleviate brain edema and IgG extravasation, treatment with amoxicillin, although significantly reducing thrombus formation, did not show significant effects in mitigating brain edema and IgG extravasation. Apparently, amoxicillin was unable to reverse the consequences of pneumonia for neutrophil recruitment and microthrombosis.

5. CONCLUSION

In summary, we observed that pneumonia following ischemic stroke impaired the recovery from stroke, with the potential mechanism being the increase in circulating neutrophils and the subsequent rise in microthrombus formation caused by pneumonia. Treatment with amoxicillin only partly alleviated the damage caused by post-stroke pneumonia during both the acute and chronic phases; depletion of neutrophils provided a more significant improvement; whereas DNase I not only failed to offer any improvement but also increased the risk of hemorrhagic transformation. Despite the fact that the use of LDC7559 indeed reduced the levels of NETs in the blood, its beneficial effects will need to be substantiated in additional studies, which are currently on the way. With the data obtained, we will be able to define if LDC7559 might represent a promising tool for improving stroke recovery in ischemic stroke patients with stroke-associated pneumonia.

6. SUMMARY

6.1. English summary

Pneumonia is one of the most common complications following ischemic stroke. It is widely recognized that stroke-associated pneumonia significantly worsens outcomes of stroke patients. However, the underlying mechanisms of its influence remain unclear.

In this study male C57Bl6/j mice underwent transient middle cerebral artery occlusion (MCAO). Three days after MCAO, mice received an intratracheal injection of bacterial suspension, containing approximately 1 x 10^8 colony-forming units (CFUs) of *Streptococcus pneumoniae* to induce pneumonia. Pneumonia significantly deteriorated neurological deficits and rotarod test performance, exacerbated brain edema and atrophy, enhanced IgG extravasation, inflammation, and microthrombosis within the infarct, and increased the neutrophil number in blood. Amoxicillin was used to treat pneumonia. Our studies showed that amoxicillin treatment attenuated the deleterious impacts of pneumonia on stroke recovery, notably diminishing the incidence of thrombi within the infarct and reducing neutrophil counts in the blood. Considering that microthrombosis is associated to neutrophils, neutrophil depletion was conducted. Neutrophil depletion more effectively improved stroke outcome than amoxicillin treatment. We also assessed the effect of DNase I and the gasdermin D inhibitor LDC7559 to prevent the formation of neutrophil extracellular traps (NETs), which are released by activated neutrophils and associated with thrombosis. DNase I treatment failed to mitigate the adverse effects of post-stroke pneumonia in the acute phase, but increased the risk of hemorrhagic transformation. LDC7559 treatment successfully reduced NET formation, microvascular thrombus, and brain edema in mice with post-stroke pneumonia.

In conclusion, post-stroke pneumonia impaired the recovery from stroke, potentially through the increase of circulating neutrophils and microthrombus formation. According to our studies, gasdermin D inhibition by LDC7559 might represent a promising strategy for the treatment of stroke-associated pneumonia.

6.2. Deutsche Zusammenfassung

Pneumonie ist eine der häufigsten Komplikationen nach einem ischämischen Schlaganfall. Es ist allgemein anerkannt, dass schlaganfall-assoziierte Pneumonie (stroke-associated pneumonia, SAP) die Ergebnisse für Schlaganfallpatienten erheblich verschlechtert. Die zugrunde liegenden Mechanismen ihres Einflusses bleiben jedoch unklar.

In dieser Studie unterzogen sich männliche C57Bl6/j Mäuse einer transienten Okklusion der mittleren zerebralen Arterie (middle cerebral artery occlusion, MCAO) für eine Dauer von 30 Minuten. Am dritten Tag nach dem Schlaganfall erhielten die Mäuse eine intratracheale Injektion einer bakteriellen Suspension, die etwa 1 x 10^8 koloniebildende Einheiten (colony-forming units, CFUs) von *Streptococcus pneumoniae* enthielt, um eine Pneumonie zu induzieren. Dies verschlechterte neurologische Defizite, Rotarod-Leistungen, Hirnödeme, Atrophie, IgG-Extravasation, Entzündungen, Mikrothrombosen und erhöhte die Neutrophilenzahlen. Amoxicillin reduzierte diese Effekte nur teilweise, darunter Thrombenbildung und Neutrophilenzahlen. In Anbetracht der Tatsache, dass Thrombosen mit Neutrophilen in Verbindung stehen, wurde eine Neutrophilendepletion durchgeführt. Die Neutrophilendepletion zeigte effektivere Verbesserungen als die Amoxicillin-Behandlung. Danach wurden DNase I und der Gasdermin D-Inhibitor LDC7559 getestet, um neutrophile extrazelluläre Traps (NETs) zu verhindern. DNase I zeigte keine Verbesserung und erhöhte das Risiko einer hämorrhagischen Transformation. Die Behandlung mit LDC7559 hingegen reduzierte erfolgreich NET-Bildung, mikrovaskuläre Thrombose und das Hirnödem.

Zusammenfassend erklärte diese Studie, dass post-Schlaganfall-Pneumonie die Erholung von Schlaganfall beeinträchtigte, sehr wahrscheinlich durch die Zunahme zirkulierender Neutrophilen und die Mikrothrombenbildung im ischämischen Gewebe. Gasdermin D-Blockade koennte eine vielversprechende Behandlung der Schlaganfall-assoziierten Pneumonie sein.

7. REFERENCES

1. Abgueguen, P., Azoulay-Dupuis, E., Noel, V., Moine, P., Rieux, V., Fantin, B. & Bedos, J. P. (2007). Amoxicillin is effective against penicillin-resistant Streptococcus pneumoniae strains in a mouse pneumonia model simulating human pharmacokinetics. *Antimicrob Agents Chemother,* 51, 208-14.
2. Albers, G. W., Marks, M. P., Kemp, S., Christensen, S., Tsai, J. P., Ortega-Gutierrez, S., Mctaggart, R. A., Torbey, M. T., Kim-Tenser, M., Leslie-Mazwi, T., Sarraj, A., Kasner, S. E., Ansari, S. A., Yeatts, S. D., Hamilton, S., Mlynash, M., Heit, J. J., Zaharchuk, G., Kim, S., Carrozzella, J., Palesch, Y. Y., Demchuk, A. M., Bammer, R., Lavori, P. W., Broderick, J. P. & Lansberg, M. G. (2018). Thrombectomy for Stroke at 6 to 16 Hours with Selection by Perfusion Imaging. *New England Journal of Medicine,* 378, 708-718.
3. Amara, N., Cooper, M. P., Voronkova, M. A., Webb, B. A., Lynch, E. M., Kollman, J. M., Ma, T., Yu, K., Lai, Z., Sangaraju, D., Kayagaki, N., Newton, K., Bogyo, M., Staben, S. T. & Dixit, V. M. (2021). Selective activation of PFKL suppresses the phagocytic oxidative burst. *Cell,* 184, 4480-4494 e15.
4. Balla, H. Z., Cao, Y. & Strom, J. O. (2021). Effect of Beta-Blockers on Stroke Outcome: A Meta-Analysis. *Clin Epidemiol,* 13, 225-236.
5. Barthels, D. & Das, H. (2020). Current advances in ischemic stroke research and therapies. *Biochim Biophys Acta Mol Basis Dis,* 1866, 165260.
6. Becker, K. J., Tanzi, P., Zierath, D. & Buckwalter, M. S. (2016). Antibodies to myelin basic protein are associated with cognitive decline after stroke. *J Neuroimmunol,* 295-296, 9-11.
7. Benjamin, E. J., Muntner, P., Alonso, A., Bittencourt, M. S., Callaway, C. W., Carson, A. P., Chamberlain, A. M., Chang, A. R., Cheng, S., Das, S. R., Delling, F. N., Djousse, L., Elkind, M. S. V., Ferguson, J. F., Fornage, M., Jordan, L. C., Khan, S. S., Kissela, B. M., Knutson, K. L., Kwan, T. W., Lackland, D. T., Lewis, T. T., Lichtman, J. H., Longenecker, C. T., Loop, M. S., Lutsey, P. L., Martin, S.

S., Matsushita, K., Moran, A. E., Mussolino, M. E., O'flaherty, M., Pandey, A., Perak, A. M., Rosamond, W. D., Roth, G. A., Sampson, U. K. A., Satou, G. M., Schroeder, E. B., Shah, S. H., Spartano, N. L., Stokes, A., Tirschwell, D. L., Tsao, C. W., Turakhia, M. P., Vanwagner, L. B., Wilkins, J. T., Wong, S. S., Virani, S. S., American Heart Association Council On, E., Prevention Statistics, C. & Stroke Statistics, S. (2019). Heart Disease and Stroke Statistics-2019 Update: A Report From the American Heart Association. *Circulation,* 139, e56-e528.

8. Bernardo-Castro, S., Sousa, J. A., Bras, A., Cecilia, C., Rodrigues, B., Almendra, L., Machado, C., Santo, G., Silva, F., Ferreira, L., Santana, I. & Sargento-Freitas, J. (2020). Pathophysiology of Blood-Brain Barrier Permeability Throughout the Different Stages of Ischemic Stroke and Its Implication on Hemorrhagic Transformation and Recovery. *Front Neurol,* 11, 594672.
9. Brinkmann, V., Reichard, U., Goosmann, C., Fauler, B., Uhlemann, Y., Weiss, D. S., Weinrauch, Y. & Zychlinsky, A. (2004). Neutrophil extracellular traps kill bacteria. *Science,* 303, 1532-5.
10. Bush, T. G., Puvanachandra, N., Horner, C. H., Polito, A., Ostenfeld, T., Svendsen, C. N., Mucke, L., Johnson, M. H. & Sofroniew, M. V. (1999). Leukocyte infiltration, neuronal degeneration, and neurite outgrowth after ablation of scar-forming, reactive astrocytes in adult transgenic mice. *Neuron,* 23, 297-308.
11. Chamorro, A., Meisel, A., Planas, A. M., Urra, X., Van De Beek, D. & Veltkamp, R. (2012). The immunology of acute stroke. *Nat Rev Neurol,* 8, 401-10.
12. Clark, W. M., Lessov, N. S., Dixon, M. P. & Eckenstein, F. (1997). Monofilament intraluminal middle cerebral artery occlusion in the mouse. *Neurol Res,* 19, 641-8.
13. Darbousset, R., Delierneux, C., Mezouar, S., Hego, A., Lecut, C., Guillaumat, I., Riederer, M. A., Evans, R. J., Dignat-George, F., Panicot-Dubois, L., Oury, C. &

Dubois, C. (2014). P2X1 expressed on polymorphonuclear neutrophils and platelets is required for thrombosis in mice. *Blood,* 124, 2575-85.

14. Darbousset, R., Thomas, G. M., Mezouar, S., Frere, C., Bonier, R., Mackman, N., Renne, T., Dignat-George, F., Dubois, C. & Panicot-Dubois, L. (2012). Tissue factor-positive neutrophils bind to injured endothelial wall and initiate thrombus formation. *Blood,* 120, 2133-43.
15. Denes, A., Pradillo, J. M., Drake, C., Sharp, A., Warn, P., Murray, K. N., Rohit, B., Dockrell, D. H., Chamberlain, J., Casbolt, H., Francis, S., Martinecz, B., Nieswandt, B., Rothwell, N. J. & Allan, S. M. (2014). Streptococcus pneumoniae worsens cerebral ischemia via interleukin 1 and platelet glycoprotein Ibalpha. *Ann Neurol,* 75, 670-83.
16. Denorme, F., Portier, I., Rustad, J. L., Cody, M. J., De Araujo, C. V., Hoki, C., Alexander, M. D., Grandhi, R., Dyer, M. R., Neal, M. D., Majersik, J. J., Yost, C. C. & Campbell, R. A. (2022). Neutrophil extracellular traps regulate ischemic stroke brain injury. *J Clin Invest,* 132.
17. Doeppner, T. R., Bretschneider, E., Doehring, M., Segura, I., Senturk, A., Acker-Palmer, A., Hasan, M. R., Elali, A., Hermann, D. M. & Bahr, M. (2011). Enhancement of endogenous neurogenesis in ephrin-B3 deficient mice after transient focal cerebral ischemia. *Acta Neuropathol,* 122, 429-42.
18. Dzyubenko, E., Manrique-Castano, D., Kleinschnitz, C., Faissner, A. & Hermann, D. M. (2018). Role of immune responses for extracellular matrix remodeling in the ischemic brain. *Ther Adv Neurol Disord,* 11, 1756286418818092.
19. Endres, M., Moro, M. A., Nolte, C. H., Dames, C., Buckwalter, M. S. & Meisel, A. (2022). Immune Pathways in Etiology, Acute Phase, and Chronic Sequelae of Ischemic Stroke. *Circ Res,* 130, 1167-1186.
20. Enlimomab Acute Stroke Trial, I. (2001). Use of anti-ICAM-1 therapy in ischemic stroke: results of the Enlimomab Acute Stroke Trial. *Neurology,* 57,

1428-34.

21. Evans, M. R. B., White, P., Cowley, P. & Werring, D. J. (2017). Revolution in acute ischaemic stroke care: a practical guide to mechanical thrombectomy. *Pract Neurol,* 17, 252-265.

22. Feigin, V. L., Stark, B. A., Johnson, C. O., Roth, G. A., Bisignano, C., Abady, G. G., Abbasifard, M., Abbasi-Kangevari, M., Abd-Allah, F., Abedi, V., Abualhasan, A., Abu-Rmeileh, N. M. E., Abushouk, A. I., Adebayo, O. M., Agarwal, G., Agasthi, P., Ahinkorah, B. O., Ahmad, S., Ahmadi, S., Ahmed Salih, Y., Aji, B., Akbarpour, S., Akinyemi, R. O., Al Hamad, H., Alahdab, F., Alif, S. M., Alipour, V., Aljunid, S. M., Almustanyir, S., Al-Raddadi, R. M., Al-Shahi Salman, R., Alvis-Guzman, N., Ancuceanu, R., Anderlini, D., Anderson, J. A., Ansar, A., Antonazzo, I. C., Arabloo, J., Ärnlöv, J., Artanti, K. D., Aryan, Z., Asgari, S., Ashraf, T., Athar, M., Atreya, A., Ausloos, M., Baig, A. A., Baltatu, O. C., Banach, M., Barboza, M. A., Barker-Collo, S. L., Bärnighausen, T. W., Barone, M. T. U., Basu, S., Bazmandegan, G., Beghi, E., Beheshti, M., Béjot, Y., Bell, A. W., Bennett, D. A., Bensenor, I. M., Bezabhe, W. M., Bezabih, Y. M., Bhagavathula, A. S., Bhardwaj, P., Bhattacharyya, K., Bijani, A., Bikbov, B., Birhanu, M. M., Boloor, A., Bonny, A., Brauer, M., Brenner, H., Bryazka, D., Butt, Z. A., Caetano Dos Santos, F. L., Campos-Nonato, I. R., Cantu-Brito, C., Carrero, J. J., Castañeda-Orjuela, C. A., Catapano, A. L., Chakraborty, P. A., Charan, J., Choudhari, S. G., Chowdhury, E. K., Chu, D.-T., Chung, S.-C., Colozza, D., Costa, V. M., Costanzo, S., Criqui, M. H., Dadras, O., Dagnew, B., Dai, X., Dalal, K., Damasceno, A. a. M., D'amico, E., Dandona, L., Dandona, R., Darega Gela, J., et al. (2021). Global, regional, and national burden of stroke and its risk factors, 1990–2019: a systematic analysis for the Global Burden of Disease Study 2019. *The Lancet Neurology,* 20, 795-820.

23. Fuchs, T. A., Brill, A., Duerschmied, D., Schatzberg, D., Monestier, M., Myers, D. D., Jr., Wrobleski, S. K., Wakefield, T. W., Hartwig, J. H. & Wagner, D. D.

(2010). Extracellular DNA traps promote thrombosis. *Proc Natl Acad Sci U S A,* 107, 15880-5.

24. Ganesh, A. & Goyal, M. (2018). Thrombectomy for Acute Ischemic Stroke: Recent Insights and Future Directions. *Curr Neurol Neurosci Rep,* 18, 59.

25. Ghelani, D. P., Kim, H. A., Zhang, S. R., Drummond, G. R., Sobey, C. G. & De Silva, T. M. (2021). Ischemic stroke and infection: A brief update on mechanisms and potential therapies. *Biochem Pharmacol,* 193, 114768.

26. Hacke, W., Kaste, M., Bluhmki, E., Brozman, M., Davalos, A., Guidetti, D., Larrue, V., Lees, K. R., Medeghri, Z., Machnig, T., Schneider, D., Von Kummer, R., Wahlgren, N., Toni, D. & Investigators, E. (2008). Thrombolysis with alteplase 3 to 4.5 hours after acute ischemic stroke. *N Engl J Med,* 359, 1317-29.

27. Hallenbeck, J. M., Dutka, A. J., Tanishima, T., Kochanek, P. M., Kumaroo, K. K., Thompson, C. B., Obrenovitch, T. P. & Contreras, T. J. (1986). Polymorphonuclear leukocyte accumulation in brain regions with low blood flow during the early postischemic period. *Stroke,* 17, 246-53.

28. Hermann, D. M. & Gunzer, M. (2019). Polymorphonuclear Neutrophils Play a Decisive Role for Brain Injury and Neurological Recovery Poststroke. *Stroke,* 50, e40-e41.

29. Herz, J., Sabellek, P., Lane, T. E., Gunzer, M., Hermann, D. M. & Doeppner, T. R. (2015). Role of Neutrophils in Exacerbation of Brain Injury After Focal Cerebral Ischemia in Hyperlipidemic Mice. *Stroke,* 46, 2916-2925.

30. Iadecola, C., Buckwalter, M. S. & Anrather, J. (2020). Immune responses to stroke: mechanisms, modulation, and therapeutic potential. *J Clin Invest,* 130, 2777-2788.

31. Iba, T. & Levy, J. H. (2018). Inflammation and thrombosis: roles of neutrophils, platelets and endothelial cells and their interactions in thrombus formation during sepsis. *J Thromb Haemost,* 16, 231-241.

32. Ito, D., Tanaka, K., Suzuki, S., Dembo, T. & Fukuuchi, Y. (2001). Enhanced

expression of Iba1, ionized calcium-binding adapter molecule 1, after transient focal cerebral ischemia in rat brain. *Stroke,* 32, 1208-15.

33. Jadhav, A. P., Desai, S. M., Kenmuir, C. L., Rocha, M., Starr, M. T., Molyneaux, B. J., Gross, B. A., Jankowitz, B. T. & Jovin, T. G. (2018). Eligibility for Endovascular Trial Enrollment in the 6- to 24-Hour Time Window: Analysis of a Single Comprehensive Stroke Center. *Stroke,* 49, 1015-1017.

34. Jagdmann, S., Berchtold, D., Gutbier, B., Witzenrath, M., Meisel, A., Meisel, C. & Dames, C. (2021). Efficacy and safety of intratracheal IFN-gamma treatment to reverse stroke-induced susceptibility to pulmonary bacterial infections. *J Neuroimmunol,* 355, 577568.

35. Jia, J., Yang, L., Chen, Y., Zheng, L., Chen, Y., Xu, Y. & Zhang, M. (2021). The Role of Microglial Phagocytosis in Ischemic Stroke. *Front Immunol,* 12, 790201.

36. Jiang, X., Andjelkovic, A. V., Zhu, L., Yang, T., Bennett, M. V. L., Chen, J., Keep, R. F. & Shi, Y. (2018). Blood-brain barrier dysfunction and recovery after ischemic stroke. *Prog Neurobiol,* 163-164, 144-171.

37. Jickling, G. C., Liu, D., Ander, B. P., Stamova, B., Zhan, X. & Sharp, F. R. (2015). Targeting Neutrophils in Ischemic Stroke: Translational Insights from Experimental Studies. *Journal of Cerebral Blood Flow & Metabolism,* 35, 888-901.

38. Kang, L., Yu, H., Yang, X., Zhu, Y., Bai, X., Wang, R., Cao, Y., Xu, H., Luo, H., Lu, L., Shi, M. J., Tian, Y., Fan, W. & Zhao, B. Q. (2020). Neutrophil extracellular traps released by neutrophils impair revascularization and vascular remodeling after stroke. *Nat Commun,* 11, 2488.

39. Kataoka, H., Kim, S. W. & Plesnila, N. (2004). Leukocyte-endothelium interactions during permanent focal cerebral ischemia in mice. *J Cereb Blood Flow Metab,* 24, 668-76.

40. Kumar, S., Selim, M. H. & Caplan, L. R. (2010). Medical complications after

stroke. *Lancet Neurol,* 9, 105-18.

41. Laridan, E., Denorme, F., Desender, L., Francois, O., Andersson, T., Deckmyn, H., Vanhoorelbeke, K. & De Meyer, S. F. (2017). Neutrophil extracellular traps in ischemic stroke thrombi. *Ann Neurol,* 82, 223-232.

42. Li, Z., Gu, M., Sun, H., Chen, X., Zhou, J. & Zhang, Y. (2023). The Potential of Gut Microbiota in Prediction of Stroke-Associated Pneumonia. *Brain Sci,* 13.

43. Liew, P. X. & Kubes, P. (2019). The Neutrophil's Role During Health and Disease. *Physiol Rev,* 99, 1223-1248.

44. Liu, D. D., Chu, S. F., Chen, C., Yang, P. F., Chen, N. H. & He, X. (2018). Research progress in stroke-induced immunodepression syndrome (SIDS) and stroke-associated pneumonia (SAP). *Neurochem Int,* 114, 42-54.

45. Lo, E. H. (2008). A new penumbra: transitioning from injury into repair after stroke. *Nat Med,* 14, 497-500.

46. Lu, Y., Li, C., Chen, Q., Liu, P., Guo, Q., Zhang, Y., Chen, X., Zhang, Y., Zhou, W., Liang, D., Zhang, Y., Sun, T., Lu, W. & Jiang, C. (2019). Microthrombus-Targeting Micelles for Neurovascular Remodeling and Enhanced Microcirculatory Perfusion in Acute Ischemic Stroke. *Adv Mater,* 31, e1808361.

47. Marsh, J. C., Boggs, D. R., Cartwright, G. E. & Wintrobe, M. M. (1967). Neutrophil kinetics in acute infection. *J Clin Invest,* 46, 1943-53.

48. Matsumoto, H., Kumon, Y., Watanabe, H., Ohnishi, T., Shudou, M., Ii, C., Takahashi, H., Imai, Y. & Tanaka, J. (2007). Antibodies to CD11b, CD68, and lectin label neutrophils rather than microglia in traumatic and ischemic brain lesions. *J Neurosci Res,* 85, 994-1009.

49. Mohamud Yusuf, A., Hagemann, N., Zhang, X., Zafar, M., Hussner, T., Bromkamp, C., Martiny, C., Tertel, T., Borger, V., Schumacher, F., Solari, F. A., Hasenberg, M., Kleinschnitz, C., Doeppner, T. R., Kleuser, B., Sickmann, A., Gunzer, M., Giebel, B., Kolesnick, R., Gulbins, E. & Hermann, D. M. (2022).

Acid sphingomyelinase deactivation post-ischemia promotes brain angiogenesis and remodeling by small extracellular vesicles. *Basic Res Cardiol,* 117, 43.

50. Moskowitz, M. A., Lo, E. H. & Iadecola, C. (2010). The science of stroke: mechanisms in search of treatments. *Neuron,* 67, 181-98.

51. National Institute of Neurological Disorders and Stroke Rt-Pa Stroke Study Group (1995). Tissue plasminogen activator for acute ischemic stroke. *N Engl J Med,* 333, 1581-7.

52. Neumann, H., Kotter, M. R. & Franklin, R. J. (2009). Debris clearance by microglia: an essential link between degeneration and regeneration. *Brain,* 132, 288-95.

53. Neumann, J., Riek-Burchardt, M., Herz, J., Doeppner, T. R., Konig, R., Hutten, H., Etemire, E., Mann, L., Klingberg, A., Fischer, T., Gortler, M. W., Heinze, H. J., Reichardt, P., Schraven, B., Hermann, D. M., Reymann, K. G. & Gunzer, M. (2015). Very-late-antigen-4 (VLA-4)-mediated brain invasion by neutrophils leads to interactions with microglia, increased ischemic injury and impaired behavior in experimental stroke. *Acta Neuropathol,* 129, 259-77.

54. Nogueira, R. G., Jadhav, A. P., Haussen, D. C., Bonafe, A., Budzik, R. F., Bhuva, P., Yavagal, D. R., Ribo, M., Cognard, C., Hanel, R. A., Sila, C. A., Hassan, A. E., Millan, M., Levy, E. I., Mitchell, P., Chen, M., English, J. D., Shah, Q. A., Silver, F. L., Pereira, V. M., Mehta, B. P., Baxter, B. W., Abraham, M. G., Cardona, P., Veznedaroglu, E., Hellinger, F. R., Feng, L., Kirmani, J. F., Lopes, D. K., Jankowitz, B. T., Frankel, M. R., Costalat, V., Vora, N. A., Yoo, A. J., Malik, A. M., Furlan, A. J., Rubiera, M., Aghaebrahim, A., Olivot, J.-M., Tekle, W. G., Shields, R., Graves, T., Lewis, R. J., Smith, W. S., Liebeskind, D. S., Saver, J. L. & Jovin, T. G. (2018). Thrombectomy 6 to 24 Hours after Stroke with a Mismatch between Deficit and Infarct. *New England Journal of Medicine,* 378, 11-21.

55. Oh, S. E. & Parikh, N. S. (2022). Recent Advances in the Impact of Infection

and Inflammation on Stroke Risk and Outcomes. *Curr Neurol Neurosci Rep,* 22, 161-170.

56. Papayannopoulos, V. (2018). Neutrophil extracellular traps in immunity and disease. *Nat Rev Immunol,* 18, 134-147.

57. Pham, M., Kleinschnitz, C., Helluy, X., Bartsch, A. J., Austinat, M., Behr, V. C., Renne, T., Nieswandt, B., Stoll, G. & Bendszus, M. (2010). Enhanced cortical reperfusion protects coagulation factor XII-deficient mice from ischemic stroke as revealed by high-field MRI. *Neuroimage,* 49, 2907-14.

58. Pircher, J., Engelmann, B., Massberg, S. & Schulz, C. (2019). Platelet-Neutrophil Crosstalk in Atherothrombosis. *Thromb Haemost,* 119, 1274-1282.

59. Schuhmann, M. K., Guthmann, J., Stoll, G., Nieswandt, B., Kraft, P. & Kleinschnitz, C. (2017). Blocking of platelet glycoprotein receptor Ib reduces "thrombo-inflammation" in mice with acute ischemic stroke. *J Neuroinflammation,* 14, 18.

60. Sharma, D., Spring, K. J. & Bhaskar, S. M. M. (2022). Role of Neutrophil-Lymphocyte Ratio in the Prognosis of Acute Ischaemic Stroke After Reperfusion Therapy: A Systematic Review and Meta-analysis. *J Cent Nerv Syst Dis,* 14, 11795735221092518.

61. Shi, K., Tian, D. C., Li, Z. G., Ducruet, A. F., Lawton, M. T. & Shi, F. D. (2019). Global brain inflammation in stroke. *Lancet Neurol,* 18, 1058-1066.

62. Singh, V., Roth, S., Llovera, G., Sadler, R., Garzetti, D., Stecher, B., Dichgans, M. & Liesz, A. (2016). Microbiota Dysbiosis Controls the Neuroinflammatory Response after Stroke. *J Neurosci,* 36, 7428-40.

63. Sollberger, G., Choidas, A., Burn, G. L., Habenberger, P., Di Lucrezia, R., Kordes, S., Menninger, S., Eickhoff, J., Nussbaumer, P., Klebl, B., Kruger, R., Herzig, A. & Zychlinsky, A. (2018). Gasdermin D plays a vital role in the generation of neutrophil extracellular traps. *Sci Immunol,* 3.

64. Stanley, D., Mason, L. J., Mackin, K. E., Srikhanta, Y. N., Lyras, D., Prakash, M. D., Nurgali, K., Venegas, A., Hill, M. D., Moore, R. J. & Wong, C. H. (2016). Translocation and dissemination of commensal bacteria in post-stroke infection. *Nat Med,* 22, 1277-1284.

65. Stojkov, D., Claus, M. J., Kozlowski, E., Oberson, K., Scharen, O. P., Benarafa, C., Yousefi, S. & Simon, H. U. (2023). NET formation is independent of gasdermin D and pyroptotic cell death. *Sci Signal,* 16, eabm0517.

66. Stoll, G. & Nieswandt, B. (2019). Thrombo-inflammation in acute ischaemic stroke - implications for treatment. *Nat Rev Neurol,* 15, 473-481.

67. Thakur, M., Junho, C. V. C., Bernhard, S. M., Schindewolf, M., Noels, H. & Doring, Y. (2023). NETs-Induced Thrombosis Impacts on Cardiovascular and Chronic Kidney Disease. *Circ Res,* 132, 933-949.

68. Tuz, A. A., Ghosh, S., Karsch, L., Ttoouli, D., Sata, S. P., Ulusoy, Ö., Kraus, A., Hoerenbaum, N., Wolf, J.-N., Lohmann, S., Zwirnlein, F., Kaygusuz, V., Lakovic, V., Tummes, H.-L., Beer, A., Gallert, M., Thiebes, S., Qefalia, A., Cibir, Z., Antler, M., Korste, S., Haj Yehia, E., Michel, L., Rassaf, T., Kaltwasser, B., Abdelrahman, H., Mohamud Yusuf, A., Wang, C., Yin, D., Haeusler, L., Lueong, S., Richter, M., Engel, D. R., Stenzel, M., Soehnlein, O., Frank, B., Solo-Nomenjanahary, M., Ho-Tin-Noé, B., Siveke, J. T., Totzeck, M., Hoffmann, D., Grüneboom, A., Hagemann, N., Hasenberg, A., Desilles, J.-P., Mazighi, M., Sickmann, A., Chen, J., Hermann, D. M., Gunzer, M. & Singh, V. (2024). Stroke and myocardial infarction induce neutrophil extracellular trap release disrupting lymphoid organ structure and immunoglobulin secretion. *Nature Cardiovascular Research*.

69. Von Bruhl, M. L., Stark, K., Steinhart, A., Chandraratne, S., Konrad, I., Lorenz, M., Khandoga, A., Tirniceriu, A., Coletti, R., Kollnberger, M., Byrne, R. A., Laitinen, I., Walch, A., Brill, A., Pfeiler, S., Manukyan, D., Braun, S., Lange, P., Riegger, J., Ware, J., Eckart, A., Haidari, S., Rudelius, M., Schulz, C., Echtler,

K., Brinkmann, V., Schwaiger, M., Preissner, K. T., Wagner, D. D., Mackman, N., Engelmann, B. & Massberg, S. (2012). Monocytes, neutrophils, and platelets cooperate to initiate and propagate venous thrombosis in mice in vivo. *J Exp Med,* 209, 819-35.

70. Wang, C., Borger, V., Sardari, M., Murke, F., Skuljec, J., Pul, R., Hagemann, N., Dzyubenko, E., Dittrich, R., Gregorius, J., Hasenberg, M., Kleinschnitz, C., Popa-Wagner, A., Doeppner, T. R., Gunzer, M., Giebel, B. & Hermann, D. M. (2020). Mesenchymal Stromal Cell-Derived Small Extracellular Vesicles Induce Ischemic Neuroprotection by Modulating Leukocytes and Specifically Neutrophils. *Stroke,* 51, 1825-1834.

71. Wang, R., Zhu, Y., Liu, Z., Chang, L., Bai, X., Kang, L., Cao, Y., Yang, X., Yu, H., Shi, M. J., Hu, Y., Fan, W. & Zhao, B. Q. (2021). Neutrophil extracellular traps promote tPA-induced brain hemorrhage via cGAS in mice with stroke. *Blood,* 138, 91-103.

72. Watcharotayangul, J., Mao, L., Xu, H., Vetri, F., Baughman, V. L., Paisansathan, C. & Pelligrino, D. A. (2012). Post-ischemic vascular adhesion protein-1 inhibition provides neuroprotection in a rat temporary middle cerebral artery occlusion model. *J Neurochem,* 123 Suppl 2, 116-24.

73. Westendorp, W. F., Dames, C., Nederkoorn, P. J. & Meisel, A. (2022). Immunodepression, Infections, and Functional Outcome in Ischemic Stroke. *Stroke,* 53, 1438-1448.

74. Westendorp, W. F., Nederkoorn, P. J., Vermeij, J. D., Dijkgraaf, M. G. & Van De Beek, D. (2011). Post-stroke infection: a systematic review and meta-analysis. *BMC Neurol,* 11, 110.

75. Westendorp, W. F., Vermeij, J.-D., Smith, C. J., Kishore, A. K., Hodsoll, J., Kalra, L., Meisel, A., Chamorro, A., Chang, J. J., Rezaei, Y., Amiri-Nikpour, M. R., Defalco, F. A., Switzer, J. A., Blacker, D. J., Dijkgraaf, M. G. W., Nederkoorn, P. J. & Van De Beek, D. (2021). Preventive antibiotic therapy in acute stroke

patients: A systematic review and meta-analysis of individual patient data of randomized controlled trials. *European Stroke Journal,* 6, 385-394.

76. Xu, C., Cai, L., Yi, T., Yi, X. & Hu, Y. (2023). Neutrophil-to-lymphocyte ratio is associated with stroke progression and functional outcome in patients with ischemic stroke. *Brain Behav*, e3261.

77. Yan, H., Kawano, T., Kanki, H., Nishiyama, K., Shimamura, M., Mochizuki, H. & Sasaki, T. (2023). Role of Polymorphonuclear Myeloid-Derived Suppressor Cells and Neutrophils in Ischemic Stroke. *J Am Heart Assoc,* 12, e028125.

78. Yin, D., Wang, C., Qi, Y., Wang, Y. C., Hagemann, N., Mohamud Yusuf, A., Dzyubenko, E., Kaltwasser, B., Tertel, T., Giebel, B., Gunzer, M., Popa-Wagner, A., Doeppner, T. R. & Hermann, D. M. (2023). Neural precursor cell delivery induces acute post-ischemic cerebroprotection, but fails to promote long-term stroke recovery in hyperlipidemic mice due to mechanisms that include pro-inflammatory responses associated with brain hemorrhages. *J Neuroinflammation,* 20, 210.

79. York, E. M., Ledue, J. M., Bernier, L. P. & Macvicar, B. A. (2018). 3DMorph Automatic Analysis of Microglial Morphology in Three Dimensions from Ex Vivo and In Vivo Imaging. *eNeuro,* 5.

80. Zec, K., Thiebes, S., Bottek, J., Siemes, D., Spangenberg, P., Trieu, D. V., Kirstein, N., Subramaniam, N., Christ, R., Klein, D., Jendrossek, V., Loose, M., Wagenlehner, F., Jablonska, J., Bracht, T., Sitek, B., Budeus, B., Klein-Hitpass, L., Theegarten, D., Shevchuk, O. & Engel, D. R. (2023). Comparative transcriptomic and proteomic signature of lung alveolar macrophages reveals the integrin CD11b as a regulatory hub during pneumococcal pneumonia infection. *Front Immunol,* 14, 1227191.

81. Zhang, R. L., Chopp, M., Jiang, N., Tang, W. X., Prostak, J., Manning, A. M. & Anderson, D. C. (1995). Anti-intercellular adhesion molecule-1 antibody reduces ischemic cell damage after transient but not permanent middle cerebral

artery occlusion in the Wistar rat. *Stroke,* 26, 1438-42; discussion 1443.

82. Zhang, X., Gong, P., Zhao, Y., Wan, T., Yuan, K., Xiong, Y., Wu, M., Zha, M., Li, Y., Jiang, T., Liu, X., Ye, R., Xie, Y. & Xu, G. (2022). Endothelial caveolin-1 regulates cerebral thrombo-inflammation in acute ischemia/reperfusion injury. *EBioMedicine,* 84, 104275.

83. Zhang, Z., Chopp, M. & Powers, C. (1997). Temporal profile of microglial response following transient (2 h) middle cerebral artery occlusion. *Brain Res,* 744, 189-98.

84. Zhao, Z., Pan, Z., Zhang, S., Ma, G., Zhang, W., Song, J., Wang, Y., Kong, L. & Du, G. (2023). Neutrophil extracellular traps: A novel target for the treatment of stroke. *Pharmacol Ther,* 241, 108328.

8. ATTACHMENT

8.1. List of abbreviations

ANOVA	analysis of variance
BBB	blood-brain barrier
CCA	common carotid artery
CD45	cluster of differentiation-45
CFUs	colony-forming units
CitH3	citrullinated histone H3
Collagen IV	collagen type IV
CXCR2	C-X-C motif chemokine receptor 2
DAMPs	damage-associated molecular patterns
dpp	days post-pneumonia
ECA	external carotid artery
GFAP	glial fibrillary acidic protein
GPIbα	glycoprotein Iba
HPA	hypothalamus-pituitary-adrenal
i.p.	intraperitoneal
i.v.	intravenous
Iba-1	ionized calcium binding adaptor molecule 1
ICA	internal carotid artery
ICAM-1	intercellular adhesion molecule 1
ICH	intracerebral hemorrhage
IL-1	interleukin 1
IQR	interquartile ranges
LDF	laser Doppler flowmetry
Ly6G	lymphocyte antigen 6 complex locus G
MCAO	middle cerebral artery occlusion

NETs	neutrophil extracellular traps
NeuN	neuronal nuclear antigen
PBS	phosphate-buffered saline
PFA	paraformaldehyde
PNS	parasympathetic nervous system
PRRs	pattern recognition receptors
ROS	reactive oxygen species
s.c.	subcutaneous
SAH	subarachnoid hemorrhage
SD	standard deviation
SNS	sympathetic nervous system
Th1	T helper cell type 1
tPA	tissue plasminogen activator
VLA-4	very-late-antigen-4

8.2. List of tables

Table 1. Equipment and materials used in surgery……... 16

Table 2. Animal allocation……17

Table 3. Modified Clark score…….. 20

Table 4. Scoring of tight rope test performance……... 25

Table 5. Antibodies and reagents used in immunohistochemistry……... 27

Table 6. Flow cytometry antibody panel…….. 31

8.3. List of figures

Figure 1. Main surgery instruments and surgical fields……..…….....15

Figure 2. Flow cytometry gating strategies…….……...… 30

Figure 3. At 2 dpp, the effects of pneumonia on neurological deficits, brain edema, and IgG extravasation, and the therapeutic efficacy of amoxicillin…….....34

Figure 4. The impact of post-stroke pneumonia on neuron survival, astrocyte reactivity, leukocyte infiltration, and ICAM-1 expression……..…….. 36
Figure 5. Post-stroke pneumonia increases microvascular thrombosis…….. 38
Figure 6. Post-stroke pneumonia reduces the number of microglia in the core of infarct, and promotes activation of microglia in both the border and core of the infarct, which are reversed by amoxicillin treatment.……...……... 40
Figure 7. Flow cytometry results of leukocytes in blood samples at 2 dpp…….42
Figure 8. Flow cytometry results of brain infiltrating leukocytes at 2 dpp…….. 43
Figure 9. Post-stroke pneumonia worsens neurological deficits mainly in the subacute stroke phase and impairs motor coordination in all phases……... 45
Figure 10. Post-stroke pneumonia exacerbates brain and striatal atrophy, and increases astrocyte reactivity……...……46
Figure 11. Neutrophil depletion mitigates infarct volume, brain edema and IgG extravasation in mice with stroke-associated pneumonia…….……....48
Figure 12. Neutrophil depletion alleviates post-ischemic microthrombosis……... 49
Figure 13. DNase I injection does not show significant effects on neurological deficits, brain volume, brain edema, and IgG extravasation in mice with post-stroke pneumonia..... 51
Figure 14. DNase I injection does not significantly reduce brain microthrombosis, but significantly increases brain hemorrhage formation…….. 52
Figure 15. LDC7559 treatment decreases the NET levels in the blood, and attenuates brain edema and IgG extravasation..... 54
Figure 16. LDC7559 injection does not influence neuronal survival and ICAM-1 expression, but significantly decreases the density of vessels with clots……...55

9. ACKNOWLEDGEMENTS

First and foremost, I would like to express my profound gratitude to my supervisor, Prof. Dirk Hermann. I am deeply thankful for the learning opportunity he has provided. Furthermore, I am very grateful to him for creating an exceptional experimental environment for me and for providing significant support in my research work through his extensive professional knowledge.

I also want to thank my colleagues, Chen Wang, Britta Kaltwasser, Yachao Qi, Nina Hagemann, Yachao Wang, Ayan Mohamud Yusuf, Maryam Sardari, Ulf Brockmeier, Mina Borbor, Egor Dzyubenko, Kristina Wagner, Xiaoni Zhang, Jing Wang, Aidong Chen, Jinhua Xue, Ying Sun, Anran Li, Xiaolong Liu, Ning Luo, Yukun Yang, Xingyun Quan, and Nihong Wu for their assistance during my research.

Furthermore, I would also like to thank our collaborators, Prof. Daniel Robert Engel, Prof. Bernd Giebel, Prof. Matthias Gunzer, PD. Jadwiga Jablonska, Stephanie Thiebes, Olga Shevchuk, Tobias Tertel, Ekaterina Pylaeva, Vikramjeet Singh, and Ali Ata Tuz for the contribution provided to our experiments.

I also want to show my gratitude to my parents and my wife for their selfless support.

Lastly, I thank all those who have helped me but have not been mentioned.

10. CURRICULUM VITAE

Der Lebenslauf ist in der Online-Version aus Gründen des Datenschutzes nicht enthalten